

6-24-2010

Studies of dielectric breakdown under pulsed power conditions

Palmarin Castro Jr

Follow this and additional works at: https://digitalrepository.unm.edu/ece_etds

Recommended Citation

Castro, Palmarin Jr. "Studies of dielectric breakdown under pulsed power conditions." (2010). https://digitalrepository.unm.edu/ece_etds/45

This Thesis is brought to you for free and open access by the Engineering ETDs at UNM Digital Repository. It has been accepted for inclusion in Electrical and Computer Engineering ETDs by an authorized administrator of UNM Digital Repository. For more information, please contact disc@unm.edu.

Palmarin A. Castro

Candidate

Electrical & Computer Engineering

Department

This thesis is approved, and it is acceptable in quality and form for publication:

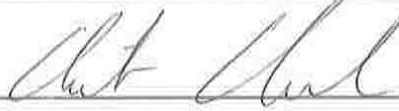
Approved by the Thesis Committee:

Dr. Edl Schamiloglu



Chairperson

Dr. Christos Christodoulou



Dr. Mark Gilmore



**STUDIES OF DIELECTRIC BREAKDOWN UNDER PULSED
POWER CONDITIONS**

BY

PALMARIN A. CASTRO

**B.S., ELECTRICAL ENGINEERING
NEW MEXICO INSTITUTE OF MINING AND
TECHNOLOGY, 1997**

THESIS

Submitted in Partial Fulfillment of the
Requirements for the Degree of

**MASTER OF SCIENCE
ELECTRICAL ENGINEERING**

The University of New Mexico
Albuquerque, New Mexico

MAY 2010

ACKNOWLEDGEMENTS

First of all, I would like to thank my advisor, Professor Edl Schamiloglu. Without his distinguished instruction and sound advice, I would not have made any progress on such a broad and difficult topic. I appreciate my group member, Professor Jerald Buchenauer, for his patience and help in my research. His rich experience in the field of pulsed power and high voltage helped me a lot during the construction of my test set up and testing. I also would like to appreciate Professor John Gaudet for his instruction and education of pulsed power and Weibull statistics in my research.

Secondly, I express my thanks to Professor Mark Gilmore for allowing me to work in his lab and use his lab facilities. Simultaneously, I would like to thank for the support from all the members in the lab of Pulsed Power, Beams, and Microwave Engineering, such as Ralph Lee Terry, and my fellow graduate students.

Finally, I appreciate my family, my wife Chassidy Dee Castro, and my daughter Jessica Castro. I will always remember the good times caring for Jessica and trying to put her to sleep while trying to write this thesis. Without the patience and encouragement of my family, it would have been impossible for me to finish my thesis. I would like to thank Dr. Bruce Freeman and Dr. Will White for reminding me every day at work that I need to finish this thesis and complete my Masters program. Also, I would like to thank Dr. Richard J. Adler and Sr. Eng. Robert Richter-Sand for setting me on this career path. I am now a more knowledgeable and complete engineer in the field of applied electromagnetics which is more than what I expected out of this career.

This work was supported by an AFOSR/DoD MURI grant on compact pulsed power.

**STUDIES OF DIELECTRIC BREAKDOWN UNDER PULSED
POWER CONDITIONS**

BY

PALMARIN A. CASTRO

ABSTRACT OF THESIS

Submitted in Partial Fulfillment of the
Requirements for the Degree of

**MASTER OF SCIENCE
ELECTRICAL ENGINEERING**

The University of New Mexico
Albuquerque, New Mexico

MAY 2010

STUDIES OF DIELECTRIC BREAKDOWN UNDER PULSED POWER

CONDITIONS

By

Palmarin Castro

B.S., Electrical Engineering, New Mexico Institute of Mining and Technology, New Mexico, 1997.

M.S., Electrical Engineering, University of New Mexico, 2010.

Abstract

In an effort to develop transmission lines with higher energy storage capabilities for compact pulsed power applications, the electrical breakdown strength (BDS) of ceramic dielectrics, particularly titanium oxide and ceramic/epoxy composite materials, are being characterized and studied. Results of research to-date show that the dense titania ceramics with nanocrystalline grain size (~200 nm) exhibit significantly higher electrical BDS as compared to ceramics made using coarse grain (micron grain size) materials when tested under DC conditions. We have performed pulsed testing under similar electric field stresses and found comparable behavior.

Furthering the research has led to find the electrical BDS of materials such as ceramic/epoxy composites. These materials seem to be more flexible, robust, and might have increased electrical BDS as compared to dense titania ceramics. The powders are available with nominal particle sizes of 50 nm to 400 nm. The crystalline ceramic powders have uniform spherical morphology, precise stoichiometry, Ba to Ti ratio, and high ceramic purity. The effects of rise time and fall time of high voltage pulsed power

on the breakdown of the ceramic/epoxy composite material will also be the focus of interest.

The purpose of this study was to describe test results, review the statistics that are used to analyze the data, and relate the understanding to what has been accumulated in the literature to-date in the context of dielectric breakdown and electrical BDS in such types of materials.

TABLE OF CONTENTS

LIST OF FIGURES	x
LIST OF TABLES	xii
CHAPTER 1: INTRODUCTION	1
CHAPTER 2: LITERATURE REVIEW	4
2.1. Introduction to Solid Material.....	4
2.2. Properties of Solid Dielectric Material	5
2.3. Electrical Breakdown of Solid Dielectric Materials	11
2.4. Two-Parameter Weibull Distribution	16
CHAPTER 3: BACKGROUND INFORMATION ON CERAMIC MATERIALS STUDIED	19
3.1. Introduction.....	19
3.2. Background Information on Ceramic Materials Studied	19
3.3. Description of Research for Dense Titania	21
3.4. Description of Research for Ceramic/Epoxy Composite Material	26
CHAPTER 4: EXPERIMENTAL SETUPS	31
4.1. Introduction	31
4.2. Experimental Setup and Procedures for Dense Titania	31
4.3. Experimental Setup and Procedures for Ceramic/Epoxy Composite Materials	35
CHAPTER 5: EXPERIMENTAL RESULTS	40
5.1. Introduction	40
5.2. Dense Titania Results	40

5.3. Mylar Results	45
5.4. Ceramic/Epoxy Composite Materials Results	46
CHAPTER 6: SUMMARY AND CONCLUSIONS	63
6.1. Summary	63
6.2. Conclusions	65
REFERENCES	69

LIST OF FIGURES

Fig. 3.1: Photograph of titanium dioxide material	21
Fig. 3.2: Sketch of a 6 coordinate titanium	23
Fig. 3.3: Breakdown strength as a function of dielectric thickness	24
Fig. 3.4: Morphology of nanocrystalline TiO ₂ as a function of sintering temperature ...	25
Fig. 3.5: Photograph of barium samples	27
Fig. 4.1: HV dielectric breakdown test setup for dense titania	32
Fig. 4.2: Photograph of chamber, transformer, and probes	33
Fig. 4.3: Photograph of the titania ceramic samples used	34
Fig. 4.4: Sketch of Mylar sample test fixture	35
Fig. 4.5: HV dielectric breakdown test set up for ceramic/epoxy composite material ...	37
Fig. 4.6: Part – BB#8 with (a) top view, and (b) side view	38
Fig. 5.1: Typical pulse waveform for dense titania	41
Fig. 5.2: Pulse waveform for dense titania during breakdown	41
Fig. 5.3: Pulse waveform for dense titania after breakdown	42
Fig. 5.4: DC breakdown test of dense titania – Weibull plot	44
Fig. 5.5: Mylar breakdown test waveform	46
Fig. 5.6: Weibull plot of the HV DC breakdown test for part – BB#3	48
Fig. 5.7: Weibull plot of the HV DC breakdown test for part – BB#4	49
Fig. 5.8: Weibull plot of the HV DC breakdown test for part – BB#6	50
Fig. 5.9: BB#8 breakdown waveforms	53
Fig. 5.10: Weibull plot of the HV DC breakdown test for part – BB#8	54
Fig. 5.11: BB#9 breakdown waveforms	55

Fig. 5.12: Weibull plot of the HV DC breakdown test for part – BB#9	56
Fig. 5.13: BB#10 breakdown waveforms	58
Fig. 5.14: Weibull plot of the HV DC breakdown test for part – BB#10	59
Fig. 5.15: BB#11 breakdown waveforms	60
Fig. 5.16: Weibull plot of the HV DC breakdown test for part – BB#11	61
Fig. 6.1: Basic Blumlein line, stacked Blumlein, folded Blumlein line	66
Fig. 6.2: Folded Blumlein line and straight Blumlein line	67

LIST OF TABLES

Table 2.1: Material values for k	15
Table 3.1: Typical physical and mechanical properties of titania	23
Table 3.2: Test sample data for part – BB#3	29
Table 3.3: Test sample data for part – BB#4	29
Table 3.4: Test sample data for part – BB#6	30
Table 5.1: Test data for dense titania	43
Table 5.2: Test sample data for part – BB#3	47
Table 5.3: Test sample data for part – BB#4	48
Table 5.4: Test sample data for part – BB#6	50
Table 5.5: Test sample data for part – BB#8	52
Table 5.6: Test sample data for part – BB#9	54
Table 5.7: Test sample data for part – BB#10	57
Table 5.8: Test sample data for part – BB#11	60

CHAPTER 1: INTRODUCTION

The study of pulsed power science and technology may be divided into four main categories: energy storage, insulation, transmission lines, and switching [1]. Each of these categories is important to the furthering of pulsed power. A successful pulsed power system cannot be achieved without addressing each of these categories.

Insulation is a critical aspect and an interesting research topic in pulsed power. Knowledge of insulation material characteristics is needed to create the best device or component with improved performance whether the application is for energy storage, transmission lines or switching. Insulation involves states of matter from solids, liquids, gases, and also plasmas. Without insulation, high voltage pulses cannot be sustained. Examples would be the use of insulation for energy storage, fine tuning of the high voltage pulses via transmission lines, and switching performance. Knowledge and correct use of insulation has the possibility of doubling the peak voltage of a pulsed power system without electrical breakdown. Increasing our knowledge of insulation through research, by the way we manipulate the characteristics of materials and the way we utilize design, there is always the possibility of designing a pulsed power machine of decreased size as compared to a present day machine that has the same input and output specifications. A good example would be folded Blumlein lines (MURI Compact Pulser research program) [2].

The characterization of electrical breakdown strengths in dielectrics, whether they are in the form of a gas, a liquid or a solid can assist in decreasing the size of pulsed power machines while increasing output. Creative things can be done with insulation to improve switches such as the use of modifying electrical fields through field

enhancement. Without the knowledge of, and continuing research into insulation characteristics, new and exciting feats in the field of pulsed power may never be achieved and the field cannot progress further. Basically, the study of insulation has been important in every aspect of state-of-the-art technology. As insulation techniques and materials improve and/or are created, so do the possibilities for application in current and future technologies.

When high voltage in pulsed power is involved, electrical breakdown is always certainly a consideration. This is a characteristic of insulating materials that needs to be understood and seems different for every type of material. There are many causes for electrical breakdown from degradation of the insulating material due to aging from the environment, the number of shots of high voltage pulses, or even just the distance of a physical gap in relation to the insulation material [1]. All this and more are crucial for consideration when trying to increase the performance of a pulsed power machine.

The characteristics of solids, particularly ceramics such as dense titania and ceramic/epoxy composite materials, and their performance under high voltage conditions is the focus of this thesis. The high dielectric constant and high voltage electrical breakdown strength are of special interest. With these special characteristics that the ceramics possess, there is a need for such materials in the realm of high voltage pulsed power. With this in mind, this will establish the basis for the MURI Compact Pulser research and explain why high voltage electrical breakdown particularly in dense titania and ceramic/epoxy composite materials is a difficult task to take on. Also, the future research of such ceramic materials can be discussed.

This thesis is divided into 6 chapters. Following this Introduction is Chapter 2, which presents a literature overview. Chapter 3 presents background information on particular ceramics studied in this research. Chapter 4 presents the experimental set-up, followed by the experimental results in Chapter 5. Chapter 6 summarizes this thesis and suggests future directions for research.

CHAPTER 2: LITERATURE REVIEW

2.1 Introduction to Solid Material

There are four common states of matter [3]. These states come in the form of a solid, liquid, gas or plasma. These states of matter exhibit very specific and noticeable characteristics in which they behave. A gas will expand to occupy its container and will maintain its shape and volume. Without a container, a gas cannot have a fixed shape or volume. A liquid, just like a gas, does not maintain a fixed shape either. A liquid also takes on the shape of its container, but unlike a gas, a liquid is not easily compressible; it requires a very large force to significantly change its volume. Gases and liquids are often referred to as fluids because they have the ability to flow and do not maintain a fixed shape. Unlike a gas and a liquid, a solid maintains a fixed shape and a fixed size. It requires a large force to change the shape and volume of a solid [4]. A plasma is a gas that is electrically conducting.

Solids can be divided into three categories. Solids can either be a conductor, an insulator, or a semiconductor. In a good conductor, electrons are bound very loosely and can move freely within the material and are often referred to as free electrons or conduction electrons. The electrons cannot leave the metal easily. When a positively charged object is brought close to or contacts a conductor, the free electrons are attracted by this positive charge and move quickly toward it. On a negatively charged object, the free electrons move swiftly away when it is brought close or makes contact. Electrons in an insulating material are bound very tightly to the nuclei and do not move about freely. Usually polarization is the result when an insulator makes contact with a charged object. An example of conduction would be two metal spheres with one highly charged and the

other electrically neutral. If an iron nail is positioned so that it makes contact with both the spheres, the previously uncharged sphere would quickly become charged. An example of insulation would be if the two spheres were connected together with a wooden rod or a piece of rubber, the electrically neutral sphere would not have become noticeably charged. Solid materials like the iron nail are said to be conductors of electricity, whereas wood and rubber are insulators [4].

Examples of good conductors are generally metals. Most other materials are insulators. Insulators also have the ability to conduct electricity very slightly. There are a few materials such as silicon, germanium, and carbon that fall into another category known as semiconductors [4]. Since the ratio $\sigma/\omega\epsilon \sim 1$ is the regime of semiconductors (here σ is the conductivity of the material, ϵ is the permittivity, and ω is the radian frequency), depending on the frequency even common material such as the damp earth (soil) can be a semiconductor.

2.2 Properties of Solid Dielectric Material

A dielectric is a term for an insulator when it is the medium between two electrodes. The difference between a conductor and a dielectric, as mentioned before, is that a conductor has loosely held electrons that can drift through its crystalline structure. In a dielectric, the electrons in the outermost shells of its atomic structure are strongly held together [5].

Electrons in materials, whether they are a conductor or a dielectric, form a symmetrical cloud around each nucleus when there is no electric field. The center of the cloud is the same location as the center of the nucleus. The electric field generated by the positively charged nucleus attracts and holds the electron cloud around it. Nuclear forces

are important, otherwise electrons would fall into the nucleus. The mutual repulsion of the electron clouds of adjacent atoms is what gives matter its form. When a conductor is subjected to an externally applied electric field, the most loosely bound electrons in each atom can jump from one lattice site to the next, thereby creating an electric current.

In a dielectric, however, an externally applied electric field cannot create an electric current since no electrons are able to move freely from one lattice site to the next [5, 6]. In terms of engineering language, it may be stated as follows: a dielectric insulator is a material that can provide high resistance to the passage of an electrical current. Generally speaking, a good insulator should have a resistivity of no less than 10^{10} ($\Omega\cdot\text{cm}$) [1]. Instead of an electric current an applied electric field can polarize the atoms or molecules in a dielectric by distorting the center of the cloud and the location of the nucleus [5]. A solid must possess several physical properties to be considered a dielectric. Being a good insulator is one property as discussed before. Polarization is another property. Solid dielectric material must have atoms or molecules that possess one or more of these five basic electric polarization types: electronic polarization, atomic or ionic polarization, dipolar polarization, spontaneous polarization, and interface or space polarization [6]. Ceramic dielectric materials have an extremely high electrical resistance preventing electron movement even when exposed to a large electrical field. This electron movement or mobility is directly related to the strength of the applied electric field and the material properties [7]. This can be seen in the equation:

$$\mathbf{u}_h = \mu_h \mathbf{E} \quad (\text{m/s}) \quad (2.2.1)$$

where \mathbf{u}_h is the electron drift velocity, μ_h is the mobility of the material or the material property, and \mathbf{E} is the applied electric field.

Polarization may be represented by an electric dipole. An electric dipole consists of a positive charge and a negative charge. The positive charge is at the center of the nucleus and the negative charge is at the center of the electron cloud. Each such dipole sets up a small electric field which points from the positively charged nucleus to the center of the equally but negatively charged electron cloud. This induced electric field is called a polarization field. It is weaker than but in the same direction as the externally applied electric field. Within a dielectric material under the influence of an applied electric field each electric dipole exhibits a dipole moment and all align themselves and the fields sum to give the polarization field. Along the upper and lower edges of a dielectric material, the dipole arrangement yields a bound negative surface charge density along the positive electrode and a bound positive surface charge density along the negative electrode [5].

Dielectric materials are not just polar materials. They may also be non-polar materials. In non-polar materials, polarization occurs only when an external electric field is applied. When the applied external electrical field is not present or taken away, the dipoles are oriented randomly and sum to yield no polarization field. In polar materials the electron cloud drifts away from the positive nucleus under an applied field in order to form a dipole. Water is an example of polar material [5, 8].

Yet another property of dielectric material is relative permittivity. It is a dimensionless quantity used to compare the permittivity of a material (ϵ_r) to the permittivity of free space (ϵ_0). The constitutive relation for a linear dielectric is:

$$D = \epsilon_r \epsilon_0 E, \quad (2.2.2)$$

where D is the electric flux density, ϵ_0 is the permittivity of free space and E is the electric field intensity. D and E are related by ϵ_0 in free space. Due to the polarization properties of a dielectric material, the presence of microscopic dipoles changes that relationship to:

$$D = \epsilon_0 E + P \quad (2.2.3)$$

where P is the electric polarization field. The electric field E produces the polarization field and polarization depends on the material properties [5, 8, 9].

A dielectric medium is linear if the magnitude of the induced polarization field is directly proportional to the magnitude of E , and is isotropic if the polarization field and E are in the same direction. In anisotropic dielectrics, E and D may have different directions.

A dielectric medium is homogeneous if the parameters ϵ , μ , and σ are constant throughout. The parameter μ is permeability and σ is conductivity. For a medium where the polarization field is directly proportional to E , the polarization field may be expressed by the relationship:

$$P = \epsilon_0 \chi_e E \quad (2.2.4)$$

where χ_e is called the electric susceptibility of the material. With careful manipulation of the electric flux density, we have:

$$D = \epsilon_0 E + \epsilon_0 \chi_e E = \epsilon_0 (1 + \chi_e) E = \epsilon E. \quad (2.2.5)$$

This defines the permittivity ϵ of the material as:

$$\epsilon = \epsilon_0 (1 + \chi_e). \quad (2.2.6)$$

It is often convenient to characterize the permittivity of a material relative to that of free space, ϵ_0 . The relative permittivity:

$$\epsilon_r = \epsilon / \epsilon_0 \quad (2.2.7)$$

where the relative permittivity is also known as the dielectric constant. In free space $\epsilon_r = 1$, for most conductors $\epsilon_r \approx 1$. The dielectric constant of air is approximately 1.0006 at sea level and decreases toward unity with increasing altitude [5, 8, 9].

Since solid, dielectric material are good insulators and have polarization, they have the ability to store energy. Depending on the configuration or shape of the two electrodes and the medium between the two electrodes, a capacitance is formed. The capacitance of a capacitor is defined as:

$$C = Q/V \quad (\text{Coulombs/ Volts or Farads}) \quad (2.2.8)$$

where C is capacitance, Q is the magnitude of the charge on the capacitor, and V is the voltage. If the configuration of the electrodes is two parallel plates with a dielectric material as the medium, the capacitance can be expressed by:

$$C = Q/V = Q/Ed = \epsilon A/d \quad (2.2.9)$$

where ϵ is the permittivity of the dielectric material, A is the area of the electrode, and d is the distance between the two plates ($d \ll A$). This is known as a parallel plate capacitor. The equation would be different for a coaxial capacitor and other configurations. Knowing the capacitance of the capacitor and the applied voltage can tell us the amount of energy stored. This is expressed by:

$$E = \frac{1}{2} CV^2 \quad (\text{units in Joules}) \quad (2.2.10)$$

where E is the energy stored in Joules, C is the capacitance, and V is the applied voltage. Manipulation of the permittivity of the dielectric material between electrodes can increase or decrease capacitance, thereby increasing or decreasing the ability to store energy.

Polarization in a dielectric material occurs to a certain extent depending on the strength of the applied electric field E . If the electric field E exceeds a certain critical value, it will free the electrons completely from the molecules and cause them to accelerate through the material in the form of a conduction current. This critical value is known as the dielectric strength of the material. When the dielectric material sustains permanent damage, due to electron collisions with the molecular structure, this is known as dielectric breakdown. The dielectric strength E_{ds} is the highest magnitude of E that the material can sustain without breakdown. Dielectric breakdown can occur in gas, liquid, and solid dielectrics. The associated field strength depends on the material composition, as well as other factors such as temperature and humidity [5, 8].

Most high power pulse applications utilize liquid or gaseous insulators mostly because breakdown in solid insulators result in irreparable damage to the insulating material whereas a breakdown in gas or liquid insulators can be cured [1].

In high voltage engineering, the maximum electric field that an insulator can withstand without breakdown is probably one of the most important factors to be concerned with. High dielectric strength increases the stored electrical energy density significantly, allowing the volume of the device to be decreased considerably. If the dielectric strength of a medium is increased by a factor of two in an energy storage capacitor, the volume of the capacitor may be reduced to one quarter of its original size. The energy density is proportional to the square of the dielectric strength [1].

The dielectric constant ϵ_r is an important property of insulating material in high voltage engineering due to the various ways in which the dielectric constant may be manipulated. It is rather broad. For example, if high energy density is required, one

should use a medium with a large dielectric constant as the energy density is directly proportional to the latter. On the other hand, if high transfer rate of energy is desired, then one should use a medium of a smaller dielectric constant as the electromagnetic wave speed is inversely proportional to the square root of ϵ .

In addition to the electrical properties in solid dielectric materials, other important properties include thermal and mechanical. Thermal and mechanical properties also play a role in how solid dielectric materials may perform under pulsed power conditions. Other failure modes besides dielectric breakdown include mechanical fracture, softening, deformation, ablation and current tracking. The ability of an insulator to survive hostile environment is crucial as failure of any one component may jeopardize the operation of a critical system [1].

2.3 Electrical Breakdown of Solid Dielectric Materials

All professionals involved in the field of pulsed power technology can agree that the field could only benefit from a greater understanding of the many complicated and varied reactions that can occur between solids used as dielectrics and also the relationship between enhancements and electrical breakdown [6, 10]. It may be possible to develop effective methods of predicting the physics and behavior of such dielectric materials such as the 3D modeling used by Schwartz in the development of dielectrics for energy storage [10]. Unfortunately predicting electrical breakdown in solids is extremely difficult.

Solid insulation forms an integral part of most high voltage facilities. The solid materials not only provide the mechanical support for the conducting parts but also insulate the conductors from one another. Therefore knowledge concerning the electrical breakdown mechanism of solid insulators is of great importance. However, the

breakdown mechanism of solids is not as well understood as breakdown in gases and liquids, although many investigations have been carried out in the past.

There are several distinct breakdown mechanisms of solids that have been identified and studied so far. They include intrinsic breakdown, streamer breakdown, thermal breakdown, erosion breakdown, breakdown due to tracking and other causes.

Intrinsic breakdown is generally considered to be due to electrons in the insulator gaining sufficient energy from the applied field to cross the forbidden energy gap from the valence band to the conduction band. Intrinsic breakdown is usually accomplished in a time scale on the order of 10^{-8} s. Streamer breakdown is conceptually similar to the streamer mechanism in gases. When the avalanche exceeds a certain critical size breakdown will occur. The transit time is usually short. Thermal breakdown occurs when an insulator is stressed electrically because of currents and dielectric losses due to polarization. If the rate of heat generation exceeds the rate of heat losses, then the insulator will undergo thermal breakdown. Such breakdown takes place usually on much longer time scales. Erosion breakdown occurs because insulators often contain voids or cavities within the material. These cavities are usually filled with gas or liquid with lower breakdown strength than that of the insulator. Accordingly, under normal working stress of the insulator the voltage across the cavities may exceed the breakdown value, hence initiating breakdown in the cavities. Breakdown due to tracking is the formation of some permanent conducting paths, usually carbon, along the insulator surface due to degradation of the insulator. Besides tracking, there are also electromechanical breakdown and treeing breakdown, etc. [1].

The breakdown of a solid insulator may arise from one or a combination of several different mechanisms mentioned previously, depending on the time duration of application of the applied field. For example, in the time range of 10^{-6} to 10^{-9} sec, breakdown of a typical solid insulator may be summarized as follows: at a very early time, intrinsic breakdown field is high. As the time of applied field extends, streamers leading to lower breakdown threshold begin to develop. At an even later time, thermal erosion and tracking take place, usually in association with repetitive charging of the insulator, where eventually breakdown finally occurs. Due to this example it can be seen how unpredictable electrical breakdown can be. Electrical breakdown can either be a short process or a very long one.

In general, high voltage pulsed systems may be direct current (dc) charged, or their high speed section can be pulsed charged. In dc charged systems the voltage can reach 12 million volts or greater. The dielectric media used for energy storage are gaseous or, at lower voltages, solid [11, 12].

Pulsed charged systems scale to higher energy at lower cost because much greater energy densities can be stored and higher electric fields can be transiently achieved than with dc charged systems [11, 12].

Designing a pulsed charged system requires breakdown criteria that can be applied to prevent breakdown in the high speed section and to achieve breakdown in the switch and requires theoretical relationships to estimate the rise time of the pulse [11, 12].

Before reviewing the individual media used in high speed sections, consider the general decrease in allowable electric field with increasing stressed area or volume. The basic point is that if the breakdown field for a given volume of solid has an intrinsic

statistical scatter, then the mean field must decrease as the volume is increased. This can be demonstrated by considering an ideal experiment in which the mean breakdown field and intrinsic standard deviation of the field of a large number of samples is known. Then sets of 10 samples are tested simultaneously and the mean breakdown voltage determined. Obviously, in any large group the unit with the lowest strength will break as a rising voltage is applied, and the new mean field will correspond to the voltage that broke only about 6.5% of the samples when they were tested individually [11, 12]. Therefore, the mean breakdown field must decrease as the volume of the sample increases, and the local rate of decrease can be calculated from the standard deviation of the unit sample breakdowns.

This, of course, assumes that measurement errors are much less than the intrinsic variations in the breakdown process. If the standard deviation is σ , then for a change of 10 in volume, the shift in mean field is just about 2σ . Thus for a σ of 12% of the mean, which is typical for solid dielectric breakdown, an increase in volume by a factor of 10 will decrease the mean breakdown field by approximately 25% and an increase in volume of 1000 will reduce the mean field for breakdown by approximately 50% [11, 12].

In the case of solids, the breakdowns originate within the volume, except possibly for thin films, so the effect depends on the volume of dielectric, not the electrode area. However, for liquids and gases the breakdowns generally originate from the electrodes, so the relevant parameter is the area of the electrodes [11, 12].

In the following, several relationships for dielectric breakdown are presented. They are accurate to 10% or 20%. Since the intrinsic scatter of solid and liquid breakdowns is about 10%, accuracies much better than that are meaningless for purposes

of design. The designer needs an accuracy of only 10% or 20% in the breakdown data for media because s/he will include a safety factor or s/he will be prepared to enlarge the system slightly after it is built [11, 12].

The designer of pulsed power systems needs the ability to calculate the breakdown voltage of dielectric systems as a function of area or volume of dielectric and for pulses of a given duration in any geometry. Pulse durations of a few microseconds to a few nanoseconds are important. Geometrical arrangements are simplified in the following discussion to uniform, mildly diverging, and point geometries [11, 12].

For solids the streamer transit times are very short. For pulse durations of at least a few nanoseconds the breakdown field is independent of the pulse duration. A practical breakdown field expression is given by:

$$E(\text{volume})^{1/10} = k, \quad (2.3.1)$$

where the field is in MV/cm and the volume is in cm³. The k is a constant where Table 2.1 shows an example of values for k for certain materials [11, 12].

Table 2.1: Material Values for k.

Materials	k
Polyethylene	2.5
Teflon	2.5
Polypropylethelene	2.9
Perspex	3.3
Mylar (thick)	3.6

For thin sheets the standard deviation of the breakdown field decreases, and the breakdown strength becomes almost independent of volume. The breakdown strength is 5.5 MV/cm, 4.0 MV/cm, and 3.0 MV/cm for 25 μm , 51 μm , and 76 μm thick sheets of Mylar, respectively [11, 12].

For diverging fields, the maximum field on the electrode and the volume stressed to more than 90% of the maximum field are used in (2.3.1) to calculate the breakdown field [11, 12].

For solids there is a reduction in breakdown field for repeated pulses given by the expression:

$$\text{Number of repetitions before breakdown} = (E_{\text{BD}} / E_{\text{op}})^8, \quad (2.3.2)$$

where E_{BD} is the breakdown field, and E_{op} is the field at which the desired number of repetitions can be obtained. The exponent in the relation in equation (2.3.2) seems to be related to the standard deviation; the exponent is 16 or greater for thin Mylar films [11, 12].

Several effects combine to alter the breakdown strength for dc charged solids and usually, but not invariably, lower it. Conduction currents can heat some plastics and cause runaway thermal degradation. Chemical corrosion from surface tracking can cause degradation of the breakdown fields, as can mechanical flow under electrostatic forces. All these effects vanish in pulse charged systems [11, 12].

2.4 Two-Parameter Weibull Distribution

The two-parameter Weibull distribution was used in this thesis work to compare the failure characteristics between solid materials studied. This was done by finding the average electrical breakdown field and the standard deviation of sample sets. Two

different types of high voltage breakdown tests were performed and the average electrical breakdown fields between the tests were also compared [13].

The two-parameter Weibull distribution will be mentioned several times in the following chapters. It is a continuous distribution that is used in a variety of situations. A common application is to model the life times of components such as ceramics, capacitors, and dielectrics [13].

The Weibull probability density function (pdf) has two parameters. Both parameters are positive constants that determine scale and shape. We denote these parameters as η and β . η is the scale parameter and β is the shape (or slope) parameter. The two-parameter Weibull probability density function (pdf) is given by:

$$f(T) = \beta/\eta (T/\eta)^{\beta-1} e^{-(T/\eta)^\beta}, \quad (2.4.1)$$

where there are the following conditions:

$$f(T) \geq 0, \quad T \geq 0, \quad \beta > 0, \quad \eta > 0. \quad (2.4.2)$$

The steps for determining the parameters of the Weibull probability density function (pdf) representing data, using probability plotting, are outlined in the following instructions. First, rank the times-to-failure in ascending order. Then obtain their median rank plotting positions. Median rank positions are used instead of other ranking methods because median ranks are at a specific confidence level (50%). Median ranks can be found tabulated in many reliability books. They can also be estimated using the following equation given by:

$$\text{Median rank} = (i - 0.3) / (N + 0.4), \quad (2.4.3)$$

where i is the failure order number and N is the total sample size. Then tabularize the times-to-failure with their corresponding median ranks. On Weibull probability paper,

plot the times and their corresponding ranks. Draw the best possible straight line through these points and obtain the slope of this line by drawing a line parallel to the one just obtained through the slope indicator on the Weibull probability paper. This value is the estimate of the shape parameter β . At the $Q(t) = 63.2\%$ ordinate point, draw a straight horizontal line until this line intersects the fitted straight line. Draw a vertical line through this intersection until it crosses the abscissa. The value at the intersection of the abscissa is the estimate of η . Now, there are values for β and η [13].

The average electrical breakdown is then calculated using the following equation given by:

$$V_b = \eta [\Gamma(1/\beta + 1)], \quad (2.4.4)$$

where η is the scale parameter and β is the shape (or slope) parameter found previously using the steps for determining the parameters of the Weibull probability density function (pdf). The following function:

$$\Gamma(1/\beta + 1) \quad (2.4.5)$$

is called the gamma function. This function, once the value is calculated, can be found in gamma function tables or calculators [13].

The standard deviation is then calculated using the following equation give by:

$$\sigma = \eta [\Gamma(2/\beta + 1) - \Gamma(1/\beta + 1)^2]^{1/2} \quad (2.4.6)$$

where η is the scale parameter, β is the shape (or slope) parameter found previously using the steps for determining the parameters of the Weibull probability density function (pdf).

CHAPTER 3: BACKGROUND INFORMATION ON CERAMIC MATERIALS STUDIED

3.1 Introduction

Ceramics can be defined as solid compounds that are formed by the application of heat and pressure, comprising at least two elements provided one of them is a non-metal or a nonmetallic elemental solid(s). A somewhat simpler definition was given by Kingery who defined ceramics as, “the art and science of making and using solid articles, which have, as their essential component, and are composed in large part of, inorganic nonmetallic materials”. In other words, what is neither metal, semiconductor, nor polymer is a ceramic [14].

For this study, the main focus are solid materials, particularly ceramics. As a class, ceramics are hard, wear-resistant, brittle, thermal shock prone, refractory, electrically and thermally insulative, intrinsically transparent, nonmagnetic, chemically stable, and oxidation-resistant. As with all generalizations, there will be exceptions; some ceramics are electrically and thermally quite conductive, while others are even superconducting. An entire industry is based on the fact that some ceramics are magnetic [14].

3.2 Background Information on Ceramic Materials Studied

Ceramics are the material of choice in high voltage applications because there are ceramic materials that have high dielectric constant and high electrical breakdown strength. Ceramics that have these characteristics need to be identified and characterized. They should be able to survive greater than 10^4 discharges. 10^4 discharges are desired because several effects combine to alter the electrical breakdown strength for DC charged

solids and usually, but not invariably, lower it. All these effects vanish in pulse-charged systems [11, 12] and new effects may arise.

Ceramic materials with high dielectric constant may lead to shorter lengths of pulse forming lines, since

$$L = ct_{\text{pulse}} / (\epsilon_r)^{1/2} \text{ (m)}. \quad (3.2.1)$$

Here L is the length of the line, c is the speed of light, t is the pulse length and ϵ_r is the dielectric constant of the medium between the plates. As the dielectric constant of the medium between the plates is increased, the length of the line is decreased.

With shorter lengths of pulse forming lines, the increase of dielectric constant leads to a more compact system. This would lower the impedance of a system since for a parallel plate line

$$Z = 377d / w (\epsilon_r)^{1/2} \text{ } (\Omega), \quad (3.2.2)$$

where Z is the impedance, d is the separation between the plates, w is the width of the plates, and ϵ_r is the dielectric constant of the medium between the plates.

Increased energy storage with no folding necessary could also be achieved since

$$W_E = 1/2 \epsilon_0 \epsilon_r E^2 \text{ (J)}, \quad (3.2.3)$$

where W_E is the energy stored, ϵ_0 is the permittivity of free space, ϵ_r is the dielectric constant of the medium between the plates, and E is the electric field. Also, ceramic materials with high electrical breakdown strengths may lead to increased energy storage [15, 16].

For the research presented in this thesis, two types of ceramic materials were studied: dense titania and ceramic/epoxy composite material. Overall, the goal is to identify a material that has a very high dielectric constant, high electrical breakdown

strength, and can survive a numerous amounts of discharges. It was found that, although the dense titania had a very high dielectric constant, the dense titania material was unreliable and difficult to manufacture in practical sizes. Even though it had increased electrical breakdown strength compared to the micron size TiO_2 , the dense titania would also breakdown at lower voltages without significant explanations. This led to the testing of material that is composite between epoxy and ceramics.

The ceramic materials provided for the study were examined closely and characterized physically. The breakdown voltage of the provided ceramic materials was then compared. Reasons for breakdown of the ceramic materials were discussed.

3.3 Description of Research for Dense Titania

Titanium dioxide, also known as titanium (IV) oxide or titania, is the naturally occurring oxide of titanium, chemical formula TiO_2 shown in Fig. 3.1 [17, 18].



Fig. 3.1: Photograph of titanium dioxide material.

An oxide is a chemical compound containing at least one oxygen atom as well as at least one other element. Most of the Earth's crust consists of oxides. Oxides result when elements are oxidized by oxygen in air [19].

The surface of most metals consists of oxides and hydroxides in the presence of air. A well known example is aluminum foil, which is coated with a thin film of aluminum oxide that passivates the metal, slowing further corrosion [19].

Due to its electronegativity, oxygen forms chemical bonds with almost all elements [19]. Oxides are usually named after the number of oxygen atoms in the oxide. Oxides containing only one oxygen are called oxides or monoxides, those containing two oxygen atoms are dioxides, three oxygen atoms makes it a trioxide, four oxygen atoms are tetroxides, and so on following the Greek numerical prefixes. Titanium dioxide (TiO_2) is an element in +4 oxidation state [19].

Titanium dioxide is noteworthy for its wide range of applications, from paint to sunscreen to food [17, 18]. Titanium dioxide occurs in nature as the well-known naturally occurring minerals rutile, anatase, and brookite; additionally, two high pressure forms, the monoclinic baddeleyite form and the orthorhombic $\alpha\text{-PbO}_2$ form have been found at the Ries crater in Bavaria. The most common form is rutile, which is also the most stable form. Anatase and brookite both convert to rutile upon heating. As seen in Fig. 3.2, Rutile, anatase, and brookite all contain 6 coordinate titanium [20].

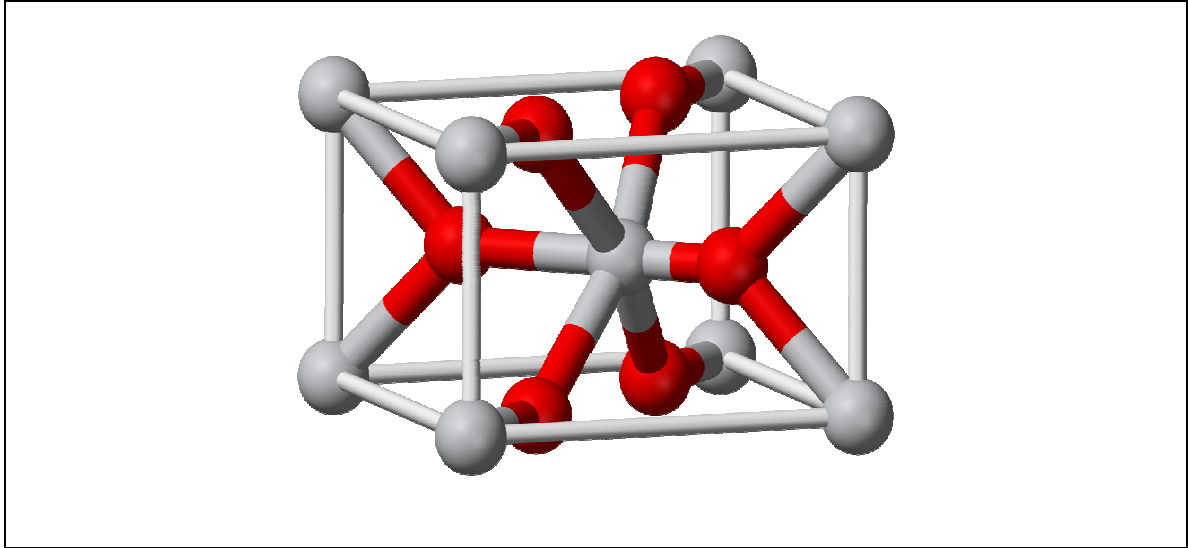


Fig. 3.2: Sketch of a 6 coordinate titanium.

The naturally occurring oxides can be mined and serve as a source for commercial titanium. The metal can also be mined from other minerals such as ilmenite or leucosene ores, or one of the purest forms, rutile beach sand. Star sapphires and rubies get their asterism from rutile impurities present in them [21].

Table 3.1: Typical physical and mechanical properties of titania.

Density	4 gcm ⁻³
Porosity	0%
Modulus of Rupture	140MPa
Compressive Strength	680MPa
Poisson's Ratio	0.27
Fracture Toughness	3.2 Mpa.m ^{-1/2}
Shear Modulus	90GPa
Modulus of Elasticity	230GPa
Micro hardness (HV0.5)	880
Resistivity (25°C)	10 ¹² ohm.cm
Resistivity (700°C)	2.5x10 ⁴ ohm.cm
Dielectric Constant (1MHz)	85
Dissipation factor (1MHz)	5x10 ⁻⁴
Dielectric strength	4 kVmm ⁻¹
Thermal expansion (RT-1000°C)	9 x 10 ⁻⁶
Thermal Conductivity (25°C)	11.7 WmK ⁻¹

Table 3.1 lists typical physical and mechanical properties of titania. It can be seen that ceramic titania has a high dielectric constant and high electrical breakdown strength.

This information shows us that it may be a viable option for use as a dielectric medium for pulsed power applications.

As the density of ceramic titania is increased, the breakdown strength will also further increase due to the removal of voids that may enhance electrical fields leading to breakdown. This material, with increased density, has the possibility to withstand high voltage and is therefore worth researching.

Previous research found that dense titania ceramics with grain size of about 200 nm exhibit significantly higher breakdown strength as compared to coarse grain ceramic materials when tested under DC conditions. This can be seen in Fig. 3.3 which exhibits higher breakdown strength in nanocrystalline TiO_2 versus micron size TiO_2 . Notice the breakdown strength as a function of dielectric thickness for nanocrystalline and coarse-grained TiO_2 [15, 16].

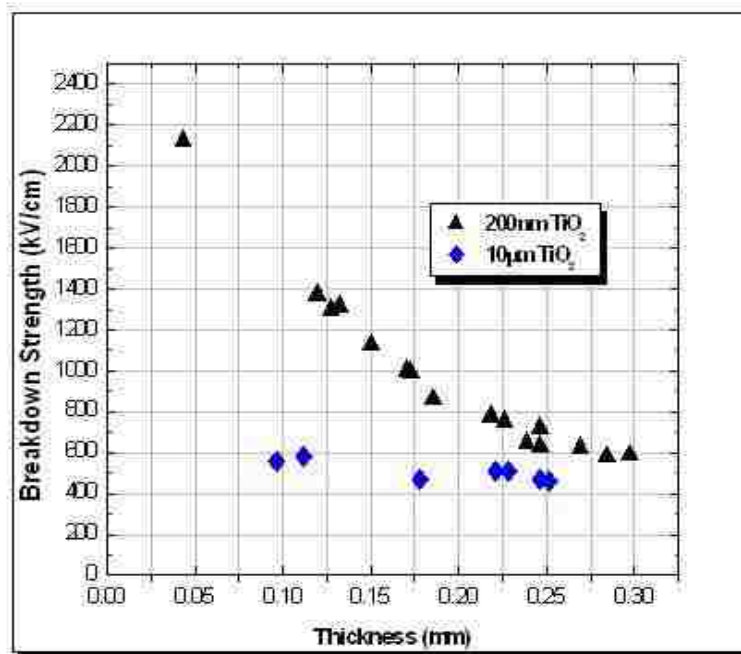


Fig. 3.3: Breakdown strength as a function of dielectric thickness.

Since grain size does make a difference in breakdown strength, Fig. 3.4 shows the morphology of nanocrystalline TiO_2 as a function of sintering temperature. 6 samples were available for pulsed testing. The samples chosen for pulsed testing were sintered at 800-850 °C because they turned out to be the smoothest or less flawed. Three samples were 6 mil thick, one sample was 6.5 mil thick, one sample was 7 mil thick, and one sample was 8.5 mil thick [15, 16].

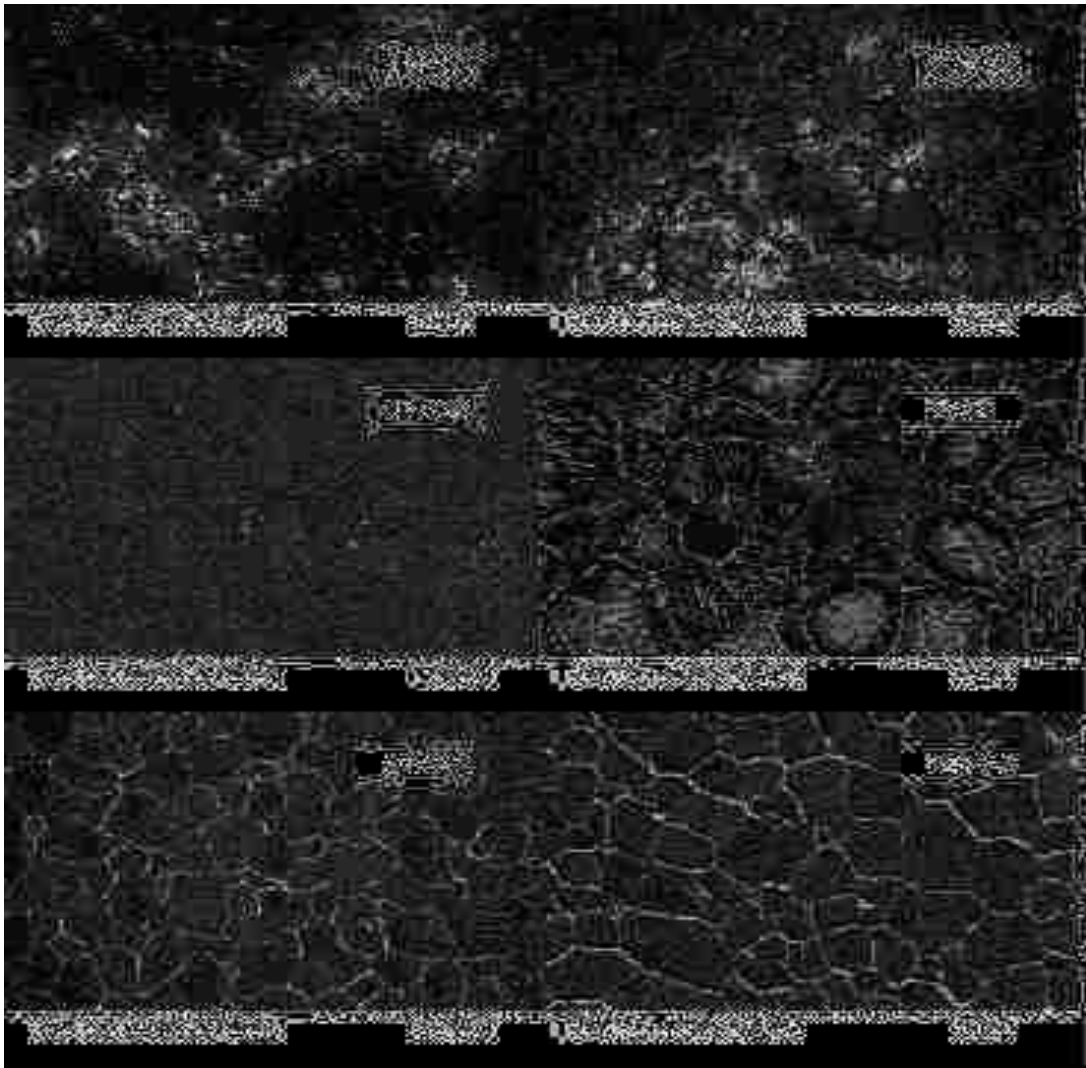


Fig. 3.4: Morphology of nanocrystalline TiO_2 as a function of sintering temperature.

3.4 Description of Research for Ceramic/Epoxy Composite Material

The ceramic/epoxy composite material provided for this study is a ratio of an epoxy which is unknown and a ceramic material which may be barium titanate. This ceramic/epoxy composite material, which has a high dielectric constant, is proprietary. A company provided the material in which we are interested in characterizing the electrical breakdown strength under pulsed charging / discharging conditions.

The sintering temperature to create the ceramic/epoxy composite material is also unknown. Although the sintering temperature is unknown, it is known that the material is not a coarse grain material. The material is a fine grain material in the nanometer size range with particle sizes that range from 50 nm to 400 nm. The crystalline ceramic powders have uniform spherical morphology, precise stoichiometry and high ceramic purity [22]. The material exhibits high breakdown strength compared to coarse grain material in the micron size range due to the decrease in voids and flaws.

Barium is a chemical element shown in Fig. 3.5. It has the symbol Ba, and atomic number 56. Barium is a soft silvery metallic alkaline earth metal. It is never found in nature in its pure form due to its reactivity with air. Its oxide is historically known as baryta but it reacts with water and carbon dioxide and is not found as a mineral. The most common naturally occurring minerals are the very insoluble barium sulfate, BaSO₄ (barite), and barium carbonate, BaCO₃ (witherite) [23, 24].



Fig. 3.5: Photograph of barium samples.

Barium is a metallic element that is chemically similar to calcium and strontium, but more reactive. This metal oxidizes very easily when exposed to air and is highly reactive with water or alcohol, producing hydrogen gas [23, 24].

Barium (Greek bary, meaning “heavy”) was first identified in 1774 by Carl Scheele and extracted in 1808 by Sir Humphry Davy in England. The oxide was at first called barote, by Guyton de Morveau, which was changed by Antoine Lavoisier to baryta, from which “barium” was derived to describe the metal [23, 24].

Barium titanate is an oxide of barium and titanium with the chemical formula BaTiO_3 . It is a ferroelectric ceramic material with photorefractive and piezoelectric properties. It has five phases as a solid, listing from high temperature to low temperature: hexagonal, cubic, tetragonal, orthorhombic, and rhombohedral crystal structure. All of the structures exhibit the ferroelectric effect except cubic [25]. It has the appearance of a white powder or transparent crystals. It is insoluble in water and soluble in concentrated sulfuric acid [25].

Barium titanate can be manufactured by liquid phase sintering of barium carbonate and titanium dioxide, optionally with other materials for doping. High purity barium titanate powder is reported to be a key component of new barium titanate capacitor energy storage systems being developed by EESstor for use in electric vehicles. Barium titanate is often mixed with strontium titanate [25].

Barium titanate is used as a dielectric material for ceramic capacitors, and as a piezoelectric material for microphones and other transducers. As a piezoelectric material, it was largely replaced by lead zirconate titanate, also known as PZT. Polycrystalline barium titanate displays positive temperature coefficient, making it a useful material for thermistors and self-regulating electric heating systems. Fully-dense nanocrystalline barium titanate has 40% higher permittivity than the same material prepared in traditional ways [26].

In characterizing the electrical breakdown strength of ceramic/epoxy composite material, many different tests can be performed. Due to the limited number of samples, the types of tests performed depend on the desired future application of the material. The company that provided the ceramic/epoxy composite material provided data in which they performed electrical breakdown strength testing. The data contained information on parts described as BB#3, BB#4, and BB#6 [16]. Each part contains 16 samples which each underwent a ramp test. The ramp test was at 20 kV/s until the material broke down.

Each sample is composed of two ball bearings which are positioned on opposite sides of the ceramic/epoxy material. The ball bearings sandwich the ceramic/epoxy material which forms a gap. The ball bearings are used as electrodes where electrical

field can be applied to test the electrical breakdown strength of the ceramic/epoxy material between the ball bearings and avoiding triple points.

Table 3.2 shows test sample data for part – BB#3 [16]. Ten samples out of 16 from part BB#3 were used. The thickness is in mils and is the measurement of the gap distance between the ball bearing electrodes. V (kV) is the voltage where breakdown occurred during the ramp test.

Table 3.2: Test sample data for part – BB#3.

Sample #	kV/mil	MV/cm	Thickness (mils)	V (kV)
1	5.91	2.33	11.5	67.99
2	6.02	2.37	11.5	69.26
3	6.33	2.49	12	75.94
4	6.40	2.52	12.5	80.02
5	6.42	2.53	13	83.48
6	6.59	2.60	12	79.11
7	6.61	2.60	12	79.34
8	6.70	2.64	13	87.10
9	6.75	2.66	10	67.49
10	6.89	2.71	12	82.67

Table 3.3 shows the test sample data for part – BB#4 [16]. Six samples out of 16 from part BB#4 were used.

Table 3.3: Test sample data for part – BB#4.

Sample #	kV/mil	MV/cm	Thickness (mils)	V (kV)
1	6.07	2.39	5.5	33.39
2	6.09	2.40	5.5	33.47
3	6.17	2.43	6	37.01
4	6.43	2.53	5.5	35.36
5	6.84	2.69	6	41.04
6	7.08	2.79	6.5	46.04

Table 3.4 shows test sample data for part – BB#6 [16]. Seven samples out of 16 from part BB#6 were used.

Table 3.4: Test sample data for part – BB#6.

Sample #	kV/mil	MV/cm	Thickness (mils)	V (kV)
1	6.07	2.39	11.5	69.78
2	6.20	2.44	12.5	77.52
3	6.23	2.45	12	74.73
4	6.45	2.54	12	77.42
5	6.57	2.59	12	78.88
6	6.76	2.66	13	87.90
7	7.29	2.87	12	87.42

Weibull statistics was used to review and compare the data (to be shown in Chapter 5). Weibull statistics is a method to characterize the probability of failure of materials due to electrical stresses. The breakdown field (MV/cm) was used in the Weibull plots [27, 28] due to differences in thickness of the ceramic/epoxy composite material between the electrodes.

The company that provided data for the ceramic/epoxy composite material that underwent ramp testing also provided four additional parts for pulsed testing. The parts were described as BB#8, BB#9, BB#10 and BB#11.

CHAPTER 4: EXPERIMENTAL SETUPS

4.1 Introduction

This chapter describes the equipment used in the experiments and the associated tests. The work was conducted at the ECE Pulsed Power, Beams and Microwaves Laboratory of the University of New Mexico. Since there were two different sets of materials, there were two experimental set-ups. Both experimental set-ups were designed to break down material and determine the voltage at which the material breaks down.

Material thickness, which determines the voltage where the material breaks down, was the leading factor for two experimental set ups. The dense titania was determined to breakdown at lower high voltage than the ceramic/epoxy materials. Figure 4.1 presents a block diagram of the experiment for dense titania.

Also, it was found that the dense titania ceramics tend to breakdown at lower electric fields under pulsed conditions compared to DC conditions. Mylar was used to test for comparison between pulsed conditions and DC conditions. The reason for testing Mylar instead of the dense titania samples for comparison between pulsed conditions and DC conditions was the limited number of dense titania samples available.

4.2 Experimental Setup and Procedures for Dense Titania

Fig. 4.1 shows a block diagram of the high voltage dielectric breakdown experimental set up to break down dense titania ceramic material. The pulsed power supply utilizes an SCR for the switch and two high voltage pulse transformers (EG&G TR-1795) to achieve the peak voltage of the pulses. The two transformers are tied to ground at the center and have a positive high side and a negative low side connecting to the electrodes where the material becomes the load. The chamber is a beaker containing

high voltage dielectric oil which harnesses the test fixture composed of the electrodes, two resistors at $220\ \Omega$ in series with the electrodes, and the dense titania material.

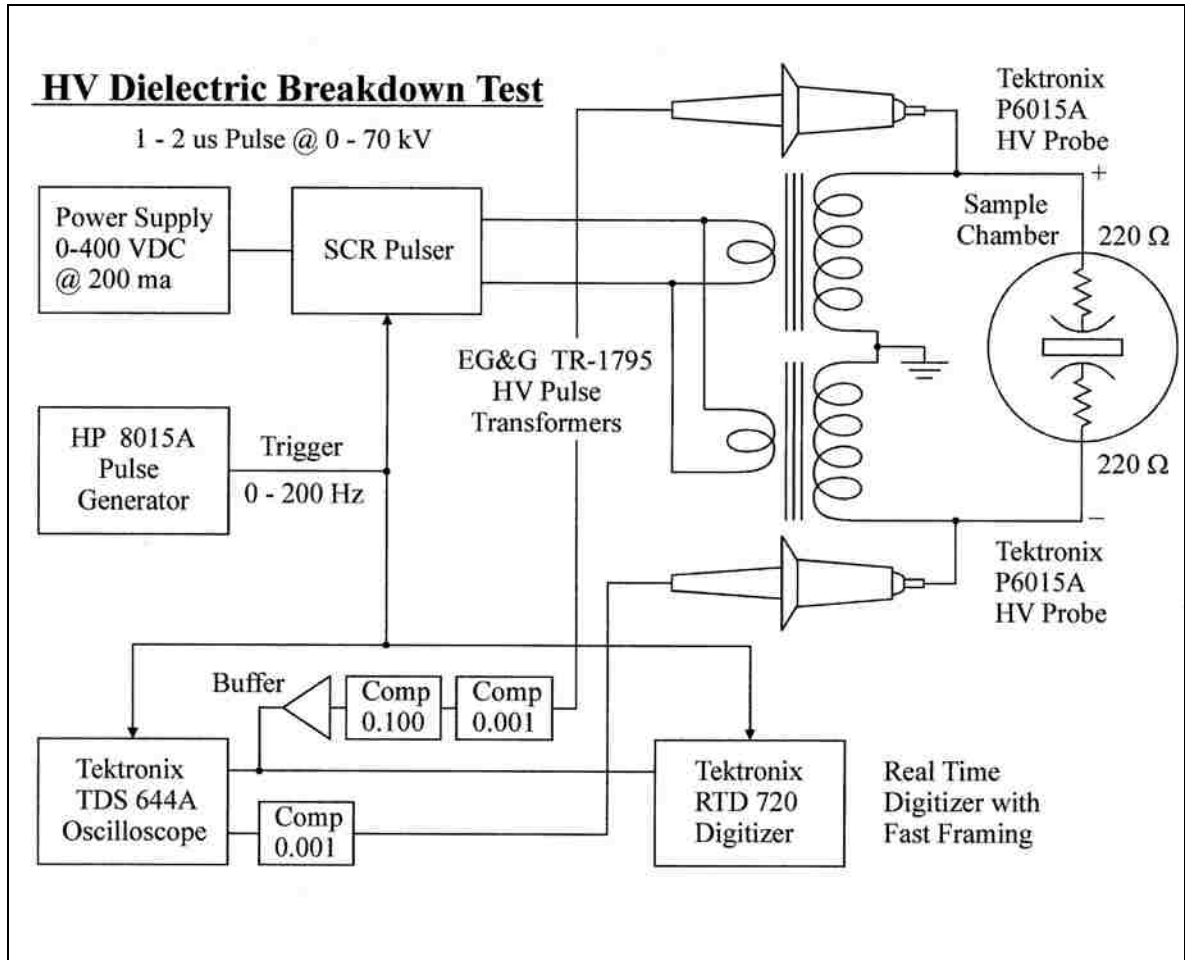


Fig. 4.1: HV dielectric breakdown test setup for dense titania.

The input consists of a 400 VDC, 2 mA power supply adjustable from 0 to 400 VDC and a HP 8015A pulse generator for the trigger adjustable up to 200 Hz. The ability to adjust the power supply from 0 to 400 VDC allows testing the dense titania material up to the voltage that the material will breakdown. The output is 0 to 70 kV maximum with a pulse width of 1 to 2 us, depending on the capacitance of the material.

Diagnostics for current measurement are not shown because voltage or breakdown strength is of interest. Current is not of interest when the material is broken down. Current is considered in providing sufficient power to break down the material. The larger the material is in thickness, the more power is needed to break down the material. This leads to the use of larger pulsed power supplies.

Fig. 4.2 shows a photograph of the chamber, two high voltage pulse transformers for positive high side and negative low side, and corresponding high voltage probes for diagnostics.



Fig. 4.2: Photograph of chamber, transformers, and probes.

A Tektronix TDS 644A oscilloscope and two Tektronix P6015A high voltage probes were used to capture waveforms. The Tektronix TDS 644A is a four channel oscilloscope with a bandwidth of 500 MHz. The Tektronix P6015A is a 1000 times probe with a rating up to 20 kV DC and 40 kV peak at a maximum of 100 ms pulse

width. The compensation range is from 7 to 49 pf. The bandwidth ranges up to 75 MHz. A Tektronix RTD 720 Digitizer was used to capture waveforms with multiple pulses.

Fig. 4.3 shows the geometry of the dense titania ceramic sample. The top portion is a sketch of the dimple where a round electrode sits. The geometry of the sample helps minimize enhanced electrical fields. This prevents any arcing around the sample so the break down occurs between the electrodes where the distance is at its minimum.

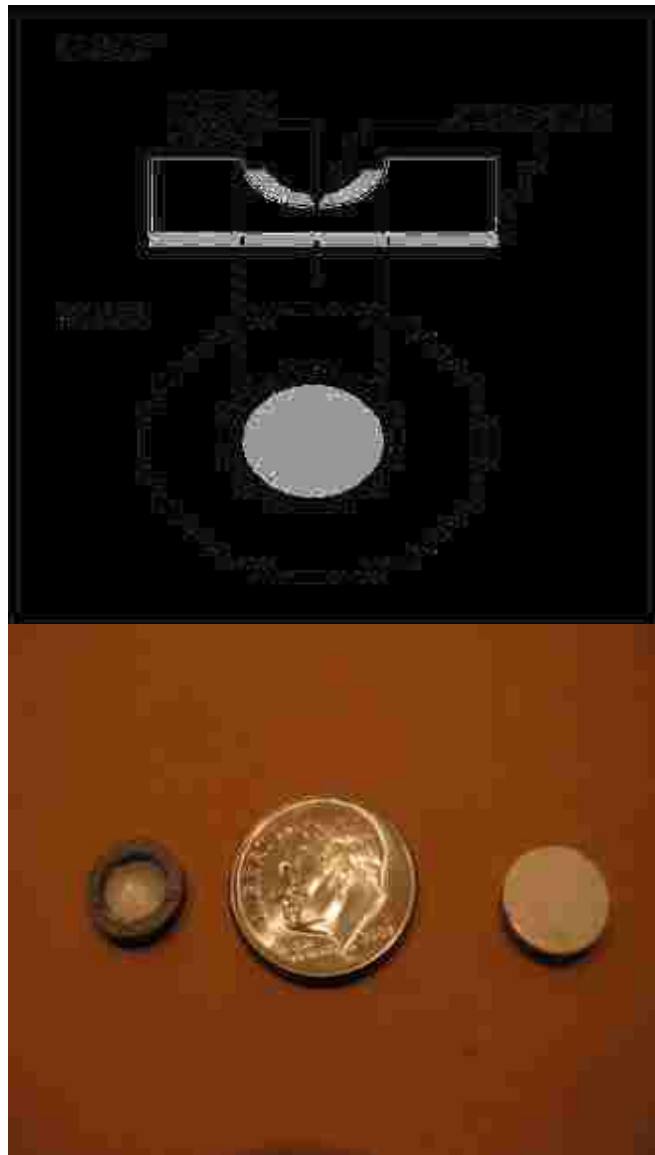


Fig. 4.3: Photograph of the titania ceramic samples used.

The sample is coated with silver where electrodes make contact. This is to increase contact with the electrodes and minimize the effects of any possible voids [15, 16].

With the dense titania material between the electrodes, the pulsed power supply is pulsed from 0 V and increased until the material reaches its breakdown strength and breaks down. The material is known to have broken down when no voltage can be seen across the electrodes. The same procedure was performed for Mylar.

Fig. 4.4 shows the sample test fixture for Mylar under the same test setup for dense titania ceramics. A Mylar square strip at 4 mils thick was placed between the electrodes and tested [15, 16].

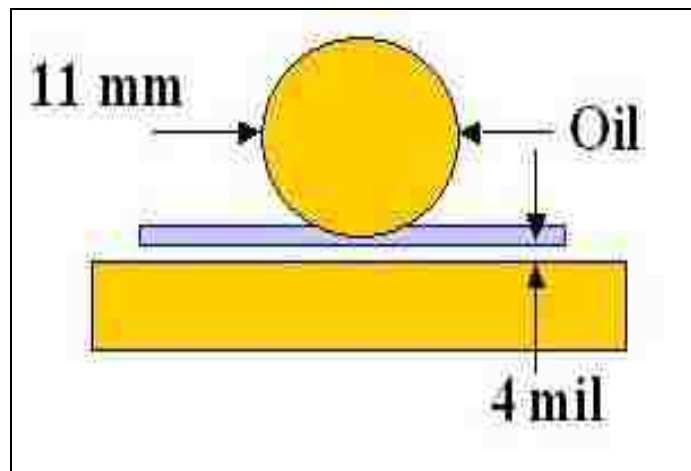


Fig. 4.4: Sketch of Mylar sample test fixture.

4.3 Experimental Setup and Procedures for Ceramic/Epoxy Composite Material

Fig. 4.6 shows a block diagram of the high voltage dielectric breakdown experimental set up to break down ceramic/epoxy composite material. The pulsed power supply utilizes a toggle switch for the switch and two ignition coils (MSD Blaster 2, MSD ignition part # 8202) to achieve the peak voltage of the pulses. The two ignition

coils are tied to ground at the center and have a positive high side and a negative low side connecting to the electrodes where the material becomes the load. The chamber is a plastic container containing high voltage dielectric oil. The chamber dimensions are 8.125 inches long, 6.5 inches wide and 5.25 inches high. The chamber harnesses the test fixture composed of the electrodes, two ignition coil wires with an impedance of 5 k Ω in series with the electrodes, and the ceramic/epoxy composite material.

The input consists of a brute force full wave rectifier circuit adjustable from 0 to 600 VDC and a toggle switch to trigger the high voltage pulse. The brute force full wave rectifier circuit plugs into 110 VAC, single phase. The circuit uses a variac that varies the 110 VAC single phase from 0 to 110 VAC. The output of the variac is then connected to a step up transformer and the full wave rectifier where VAC is rectified to VDC. The maximum voltage is 600 VDC. The voltage is then smoothed out with two 100 μ F capacitors in series. Resistors with a value of 100 k Ω are across the 100 μ F capacitors to bleed off energy when the circuit is de-energized. Two 250 k Ω resistors in series are used to limit current to the ignition coils when switched by the toggle switch. The toggle switch is wired up in a fashion so that the brute force full wave rectifier circuit charges up two 1 μ F capacitors in parallel up to the desired voltage. When the toggle switch is switched, the toggle switch will release the energy from the 1 μ F capacitors in parallel. The energy is then released to the ignition coils where the voltage is stepped up dramatically. An LC circuit is basically being used to break down the ceramic/epoxy composite material.

The ability to adjust the power supply from 0 to 600 VDC allows testing the ceramic/epoxy composite material up to the voltage that the material will break down.

The output is 0 to over 100 kV with a pulse width of approximately 100 us, depending on the capacitance of the material.



Fig. 4.5: HV dielectric breakdown test setup for ceramic/epoxy composite material.

A Tektronix TDS 644A oscilloscope and two North Star high voltage probes (Part # PVM-1) were used to capture waveforms. The Tektronix TDS 644A is a four channel oscilloscope with a bandwidth of 500 Mhz. The PVM-1 is a 1000 times probe with a rating up to 40 kV DC and 60 kV peak. The bandwidth ranges up to 80 MHz.

This ceramic/epoxy composite material, which has a high dielectric constant, is proprietary in which the nature cannot be disclosed. A company provided the material in

which we are interested in characterizing the electrical breakdown strength under pulsed charging / discharging conditions.

Precision ball bearings were used as the electrodes to help minimize electrical field enhancement that would create surface flashover [11, 12]. One part consists of 16 samples with the electrodes attached to the ceramic/epoxy composite materials. Figure 4.6 shows photographs of the sample part-BB#8 [16].

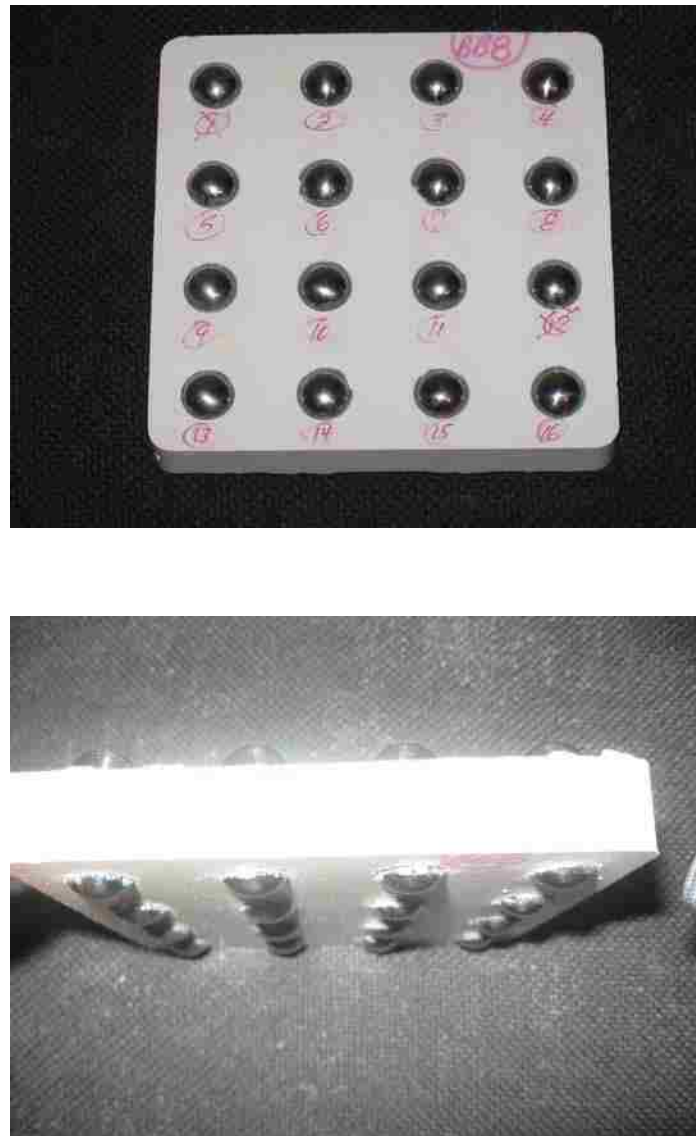


Fig. 4.6: Part – BB#8 with (a) top view, and (b) side view.

When testing, the material would be immersed in high voltage dielectric oil to prevent arcing between the bearings since the bearings are close together and voltages would reach in the realm of 80 kV. There is a gap between the electrodes where the thickness is calculated through measurements. When the ceramic/epoxy composite material was made, the ball bearings were temporarily glued to a fixture to create the gap between the precision ball bearings.

In characterizing the electrical breakdown strength of the ceramic/epoxy composite material, there are many different tests that can be performed. Due to the limited number of samples, the types of tests performed depended on the desired future application of the material. Voltage pulsed tests were performed on the ceramic/epoxy composite materials where the rise times were typically in the order of 75 us. The voltage pulsed tests basically consisted of setting the input voltage to maximum and switching the toggle switch. The output voltage increases until the ceramic/epoxy composite material breaks down. The voltage at which the material breaks down is then recorded.

CHAPTER 5: EXPERIMENTAL RESULTS

5.1 Introduction

It is known that coarse grain titania (micron size grains) will break down at a lower voltage than dense titania (nanometer size grains) with the same thickness or gap distance between electrodes under high voltage DC testing. Dense titania exhibit significantly higher breakdown strength.

As for ceramic/epoxy composite material, the company that provided the material also provided data in which they performed electrical breakdown strength testing. The testing was DC ramp testing at 20 kV/s until the material broke down.

A comparison of data for dense titania and ceramic/epoxy composite material, in which high voltage DC ramp tests were performed, showed that the ceramic/epoxy composite material exhibit significantly higher breakdown strength. The electrical breakdown strength for dense titania is 0.728 MV/cm as compared to ceramic/epoxy composite material which is 2.55 MV/cm.

This chapter will present the data taken from high voltage pulsed testing performed on dense titania and ceramic/epoxy composite material.

5.2 Dense Titania Results

Fig. 5.1 shows a typical pulse waveform for dense titania. The pulsed power supply voltage is increased from 0 V to 12.5 kV. The waveform shows that the pulse has a peak voltage of 12.5 kV. The rise time is about 1 μ s. The pulse width is about 5 μ s and shows a droop that occurs quickly as soon as the peak voltage is achieved. The droop is about 2 μ s in length. There is no breakdown to be observed at this point.

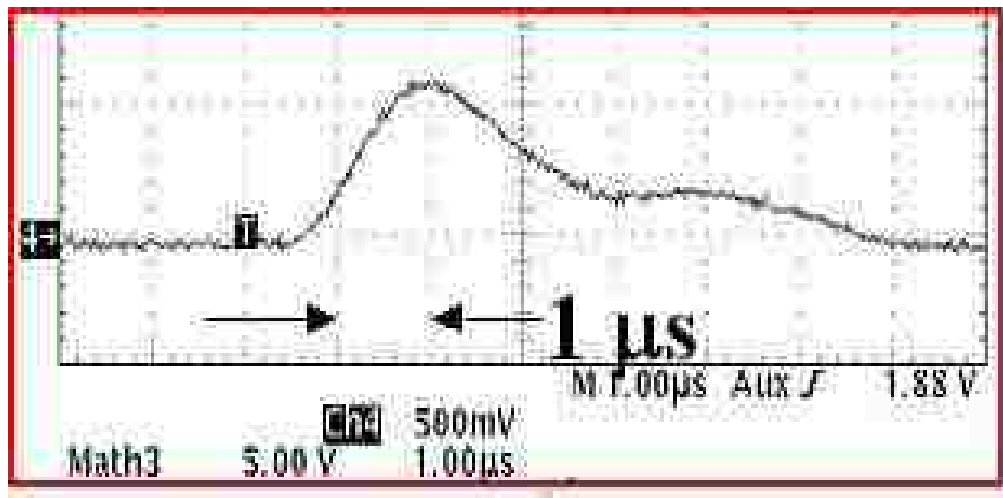


Fig. 5.1: Typical pulse waveform for dense titania.

The pulsed power supply voltage is then increased from 0 V to 13.5 kV for another shot. Fig. 5.2 shows a pulse waveform during breakdown. The waveform shows that the pulse has a peak voltage of 13.5 kV and the rise time is about 1 μ s. Breakdown can be shown on the falling edge of the pulse. The fall time of the breakdown can be approximated to be 100 ns.

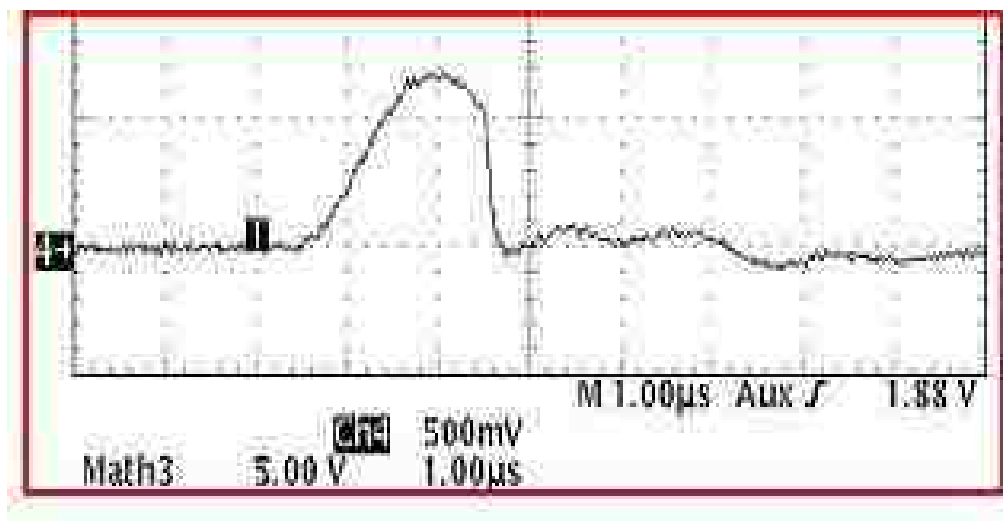


Fig. 5.2: Pulse waveform for dense titania during breakdown.

After breakdown has occurred, yet another shot was taken. Fig. 5.3 shows the pulse waveform after breakdown. Voltage cannot be sustained across the electrodes [15, 16].

The waveforms show voltage behavior before, during, and after breakdown has occurred in dense titania. The waveforms came in handy when trying to determine when breakdown occurred in each sample under test.

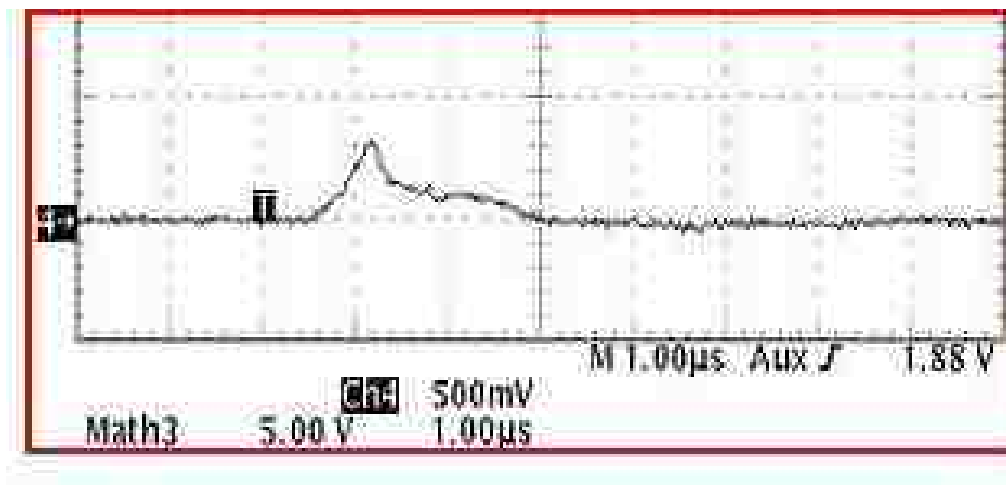


Fig. 5.3: Pulse waveform for dense titania after breakdown.

Table 5.1 shows 6 samples of dense titania that were subjected to high voltage DC tests and high voltage pulse tests. Although only 6 samples were tested, hardly enough to come to a solid conclusion, results show that breakdown strength may be lower during pulsed conditions than DC conditions. This possibility is also seen in Table 5.1 [15, 16].

Table 5.1: Test data for dense titania.

Sample Number	Sintering Temp.	Thickness (mils)	Status (Break/Survive)
1	800° C	6.5	*DC: 10 kV *Pulsed: 4.8 kV
2	800° C	6.0	DC: 14 kV Pulsed: -
3	800° C	6.0	DC: 7.5 kV Pulsed: -
4	850° C	7.0	DC: 18 kV Pulsed: 13.5 kV
5	850° C	8.5	*DC: 16 kV *Pulsed: 17 kV
6	850° C	6.0	DC: 11.5 kV Pulsed: -

With the results from the 6 samples taken, a Weibull plot for DC breakdown for dense titania was created. Fig. 5.4 show the DC breakdown test of TiO₂ nanocrystalline ceramic [15, 16]. It shows that the average breakdown voltage was 11.1 kV and the electrical breakdown strength is 0.728 MV/cm. The dense titania samples used in the Weibull plot all had a thickness of 6.0 mils between the electrodes. More samples may have led to a better conclusion.

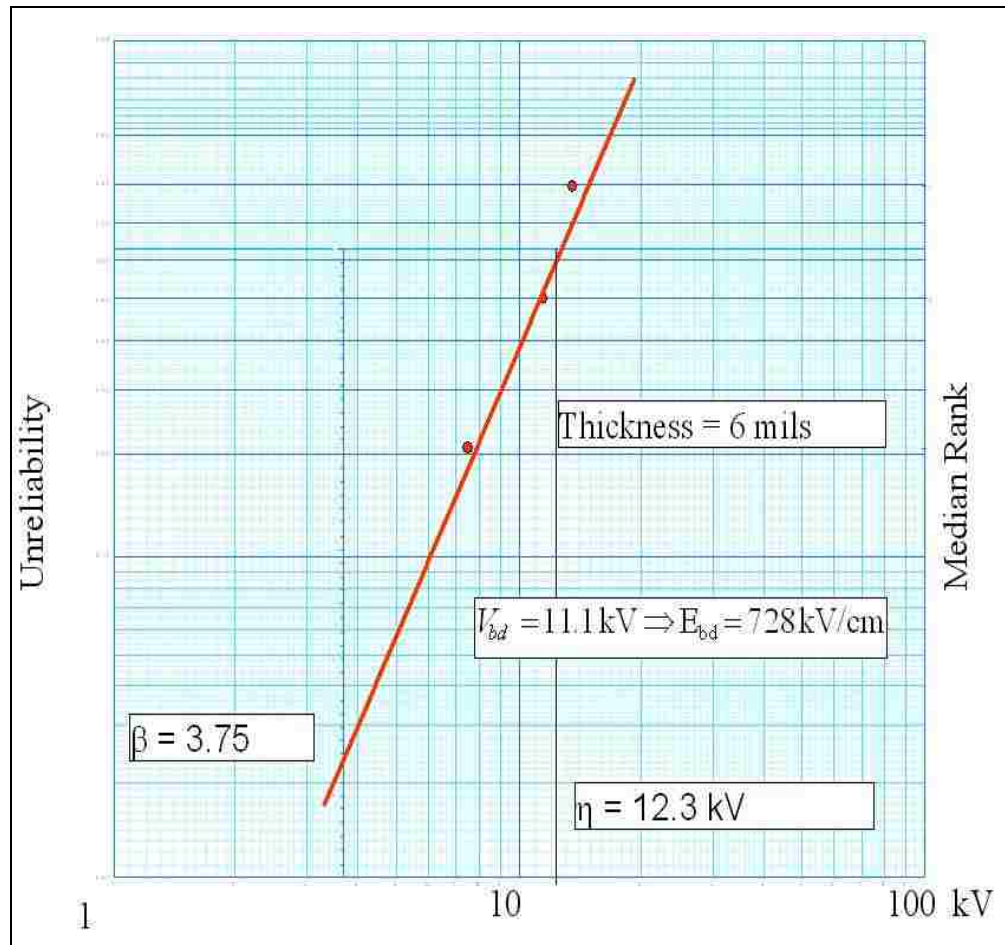


Fig. 5.4: DC breakdown test of dense titania – Weibull plot.

As for data for dense titania subjected to pulsed testing, a Weibull plot was not created because only two data points were available. The two available data points are 13.5 kV breakdown at 7.0 mils thickness between electrodes and 17 kV breakdown at 8.5 mils thickness between electrodes. This is shown in Table 5.1. The electrical breakdown field is 1.93 kV/mil or 0.76 MV/cm for breakdown at 13.5 kV. The electrical breakdown field is 2 kV/mil or 0.79 MV/cm for breakdown at 17 kV. Again, more samples may have led to a better conclusion. Weibull statistics could have been used if additional data points were taken.

Since Weibull statistics could not be used for the data for dense titania subjected to pulsed testing, the electrical breakdown field strength for dense titania subjected to DC breakdown tests and electrical breakdown field strength for dense titania subjected to pulsed breakdown tests could not be easily compared. Also, the thicknesses between the electrodes for dense titania subjected to pulsed breakdown tests are greater than the electrodes for dense titania subjected to DC breakdown tests. Sample thicknesses were not the same. More samples for pulsed breakdown testing would have given better results where different thicknesses were involved. At 8.5 mil thickness, the breakdown field is 0.79 MV/cm for dense titania under pulsed breakdown tests as compared to 0.728 MV/cm breakdown field at 6.0 mil thickness for dense titania under DC breakdown tests.

At first glance, the data seems to show that breakdown strength is greater under pulsed conditions than DC conditions. It was concluded that dense titania ceramics may tend to breakdown at lower electric fields under pulsed conditions than DC conditions.

5.3 Mylar Results

Since findings show that dense titania ceramics tend to breakdown at lower electric fields under pulsed conditions compared to DC conditions (approximately 25% lower), we had to digress from testing ceramic materials and test Mylar. We wanted to see if the observations with dense titania are repeatable with Mylar.

Samples of untested Mylar at 4 mils thick were used. 25 shots per burst were used as the pulsed power supply was slowly ramped up from 0 V until the Mylar reached its breakdown strength.

A Mylar sample was pulsed at 16 kV. After 1000 shots at 100 Hz, there was no breakdown. A second sample was pulsed at 17 kV. After 700 shots at 100 Hz,

breakdown occurred. A third sample was pulsed at 18 kV. After 12 shots at 100 Hz, breakdown occurred. A fourth sample was pulsed at 20 kV. It took a single pulse for breakdown to occur. Fig. 5.5 shows a test waveform where at 18 kV there was breakdown on shot number 12 [15, 16].

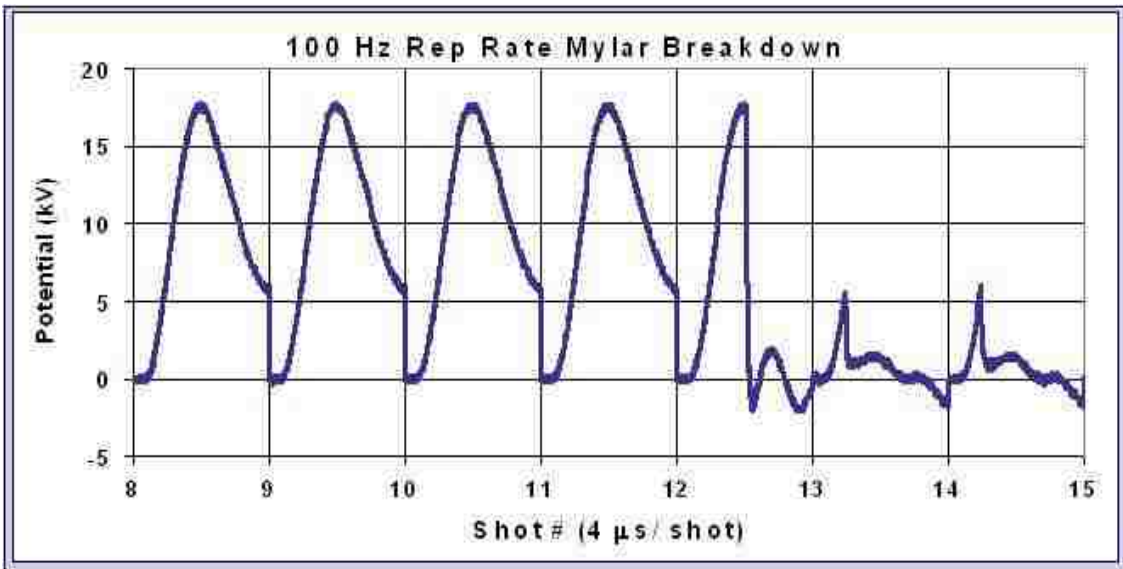


Fig. 5.5: Mylar breakdown test waveform.

The Mylar was then tested with a DC power supply. The DC power supply was slowly ramped up from 0V to 26 kV where it reached its breakdown strength and breakdown occurred.

After performing both high voltage pulsed power tests and high voltage DC tests on mylar, it can be concluded that breakdown occurs at lower voltages under pulsed power conditions as compared to DC. This is consistent with the data.

5.4 Ceramic/Epoxy Composite Materials Results

In characterizing the electrical breakdown strength of ceramic/epoxy composite material, we first take a look at the data which was provided to us. The data contained

information on parts – BB#3, BB#4, and BB#6. Each part contained 16 samples which underwent a ramp test. The ramp test was at 20 kV/s until the material broke down.

Table 5.2 shows test sample data for part – BB#3 [16]. Using Weibull statistics with the maximum likelihood estimator [27, 28], the average breakdown field is approximately 2.55 MV/cm and the standard deviation is approximately 0.12 MV/cm.

Table 5.2: Test sample data for part – BB#3.

Sample #	kV/mil	MV/cm	Thickness (mils)	V (kV)
1	5.91	2.33	11.5	67.99
2	6.02	2.37	11.5	69.26
3	6.33	2.49	12	75.94
4	6.40	2.52	12.5	80.02
5	6.42	2.53	13	83.48
6	6.59	2.60	12	79.11
7	6.61	2.60	12	79.34
8	6.70	2.64	13	87.10
9	6.75	2.66	10	67.49
10	6.89	2.71	12	82.67

Fig. 5.6 shows the Weibull plot of the high voltage DC breakdown test of ceramic/epoxy composite material part - BB#3. The data shows an excellent fit to the Weibull 2-parameter function [16].

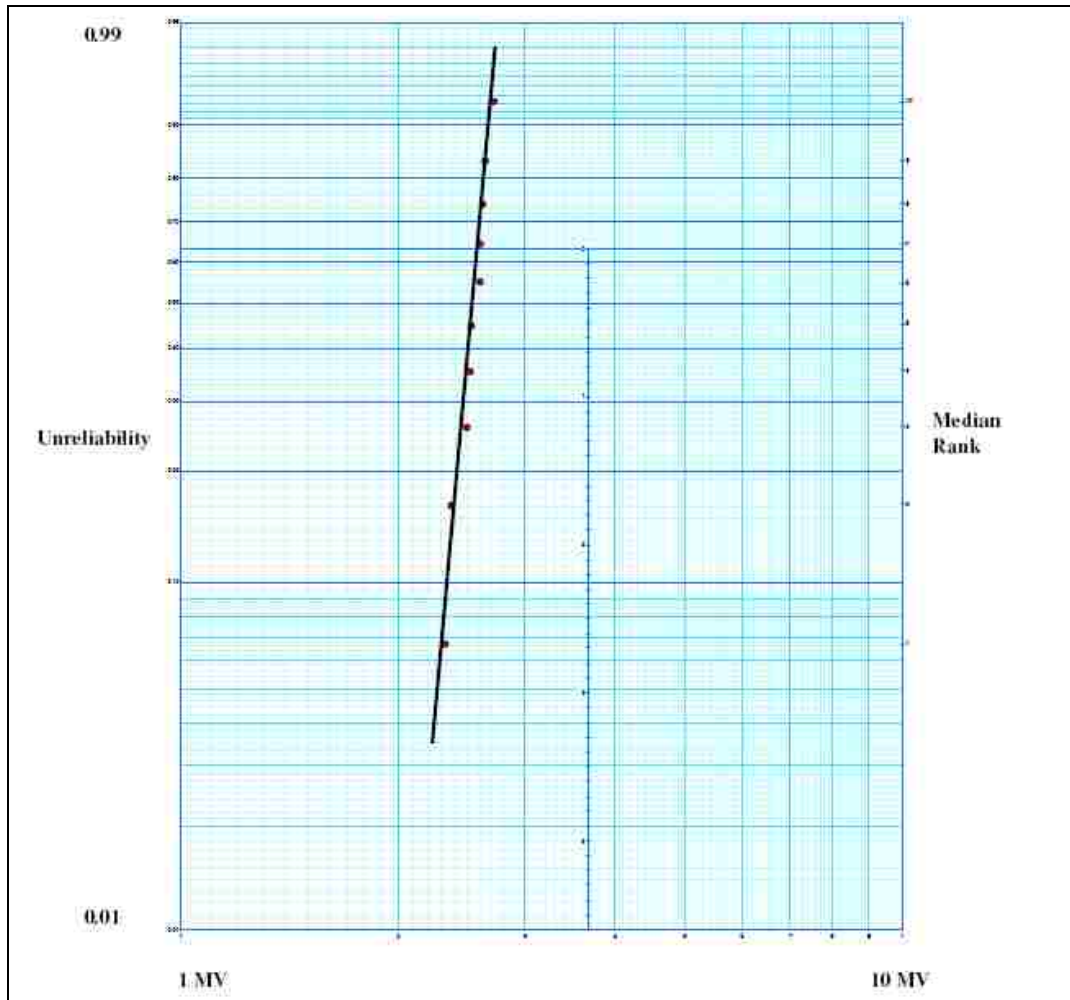


Fig. 5.6: Weibull plot of the HV DC breakdown test for part – BB#3.

Table 5.3 shows test sample data for part – BB#4 [16]. The average breakdown field is now approximately 2.53 MV/cm and the standard deviation was approximately 0.18 MV/cm.

Table 5.3: Test sample data for part – BB#4.

Sample #	kV/mil	MV/cm	Thickness (mils)	V (kV)
1	6.07	2.39	5.5	33.39
2	6.09	2.40	5.5	33.47
3	6.17	2.43	6	37.01
4	6.43	2.53	5.5	35.36
5	6.84	2.69	6	41.04
6	7.08	2.79	6.5	46.04

Fig. 5.7 shows the Weibull plot of the high voltage DC breakdown test of ceramic/epoxy composite material part - BB#4 [16].

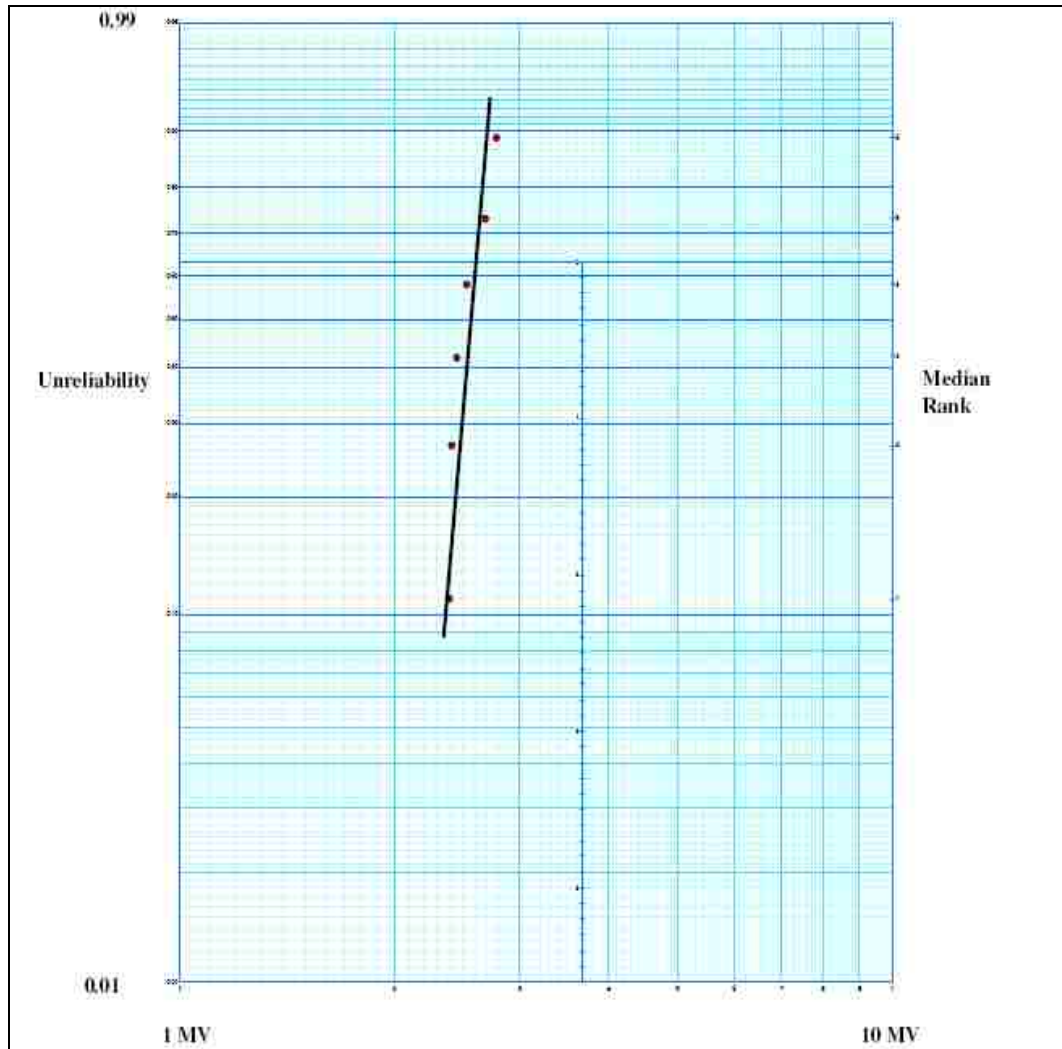


Fig. 5.7: Weibull plot of the HV DC breakdown test for part – BB#4.

Table 5.4 shows the test data for part – BB#6 [16]. The average breakdown field is the same as the previous sample, 2.55 MV/cm with a standard deviation of approximately 0.20 MV/cm.

Table 5.4: Test sample data for part – BB#6.

Sample #	kV/mil	MV/cm	Thickness (mils)	V (kV)
1	6.07	2.39	11.5	69.78
2	6.20	2.44	12.5	77.52
3	6.23	2.45	12	74.73
4	6.45	2.54	12	77.42
5	6.57	2.59	12	78.88
6	6.76	2.66	13	87.90
7	7.29	2.87	12	87.42

Fig. 5.8 shows the goodness of the fit with the Weibull function [16].

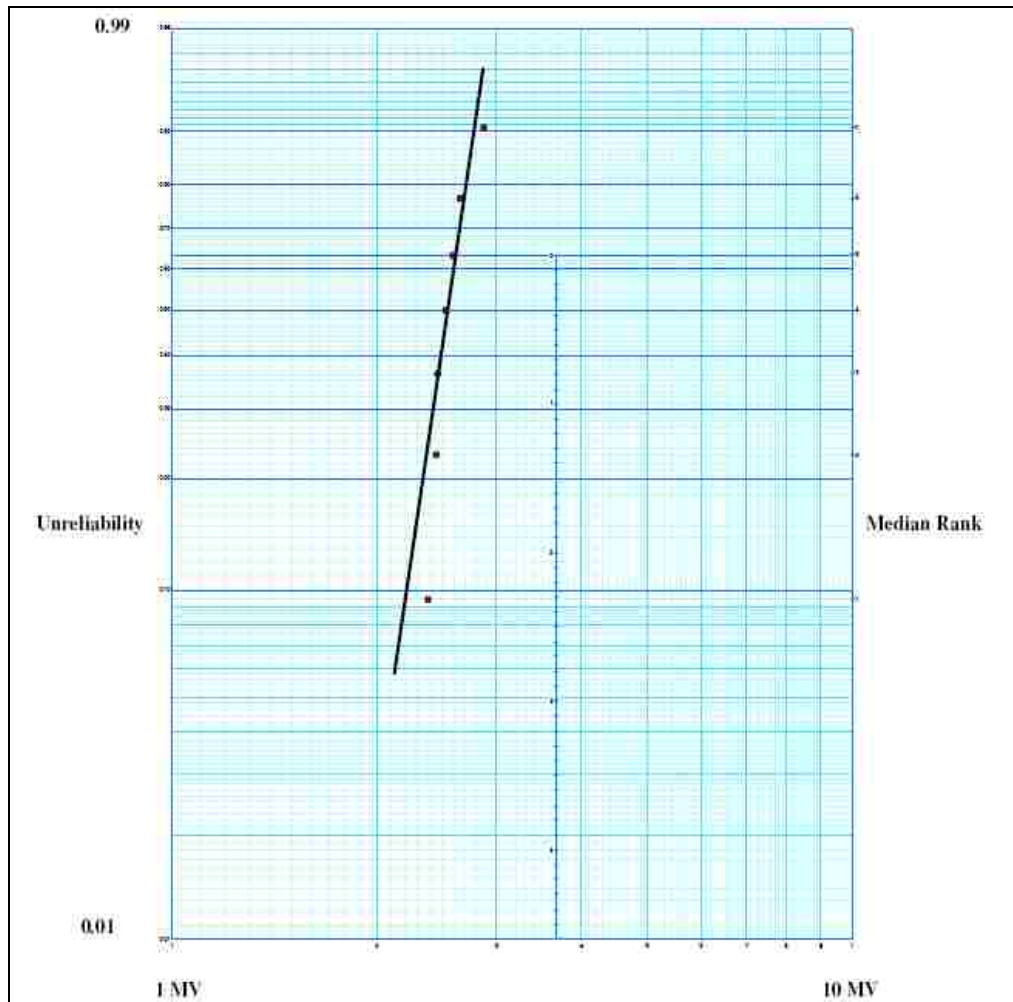


Fig. 5.8: Weibull plot of the HV DC breakdown test for part – BB#6.

The small standard deviation for each part shows that the ceramic/epoxy composite material breaks down consistently at a critical electrical field. The steepness of the slope (β) indicates the likelihood of failure increases rapidly as the electric field applied to the sample gets larger.

With the data combined considering the different thickness between the precision ball bearings (gap distance containing the ceramic/epoxy composite material), it was calculated that the average electrical field breakdown was 6.47 kV/mil with a deviation of 0.36 kV/mil or 2.55 MV/cm with a deviation of 0.14 MV/cm [16].

After we have taken a look at the data in which the ceramic/epoxy composite material underwent a ramp test, we now pay attention to the four parts that were given to us for pulsed power testing. The parts were described as parts – BB#8, BB#9, BB#10, and BB#11. The pulsed power test involved subjecting the ceramic/epoxy composite sample to a high voltage pulse until the material across the ball bearings broke down. The ball bearings are the electrodes. At this point, the impedance across the electrodes should be very low due to carbon formations from breakdown. A high voltage pulse can no longer be sustained or established.

Table 5.5 shows test sample data for part – BB#8. Seven samples out of 16 were good data points. Using Weibull statistics with the maximum likelihood estimator [27, 28], the average breakdown field is approximately 0.93 MV/cm and the standard deviation is approximately 0.13 MV/cm.

Table 5.5: Test sample data for part – BB#8.

Rank	Sample #	kV/mil	MV/cm	Thickness (mils)	V (kV)
1	15	1.77	0.70	13	23
2	7	2.22	0.87	12	26.6
3	14	2.4	0.94	12.5	28
4	11	2.4	0.94	12	28.8
5	13	2.5	0.98	12	30
6	9	2.48	0.98	12.5	31
7	10	2.92	1.15	12	35

Fig. 5.9 shows breakdown waveforms for part – BB#8. The rise times for each sample are very similar and follow an LC tank circuit until the sample breaks down. Inductance remains the same for each test and is constant. The capacitance is different for each sample because the gap distance between the electrodes of each sample is different. The capacitance for each sample is unknown and was not measured. Though we do not know the capacitance, we can see from the rise time that the capacitance values must be very close between samples. Notice sample #10 appears to not have broken down. This is not the case. An additional shot was taken on sample #10 and the sample did not hold any voltage.

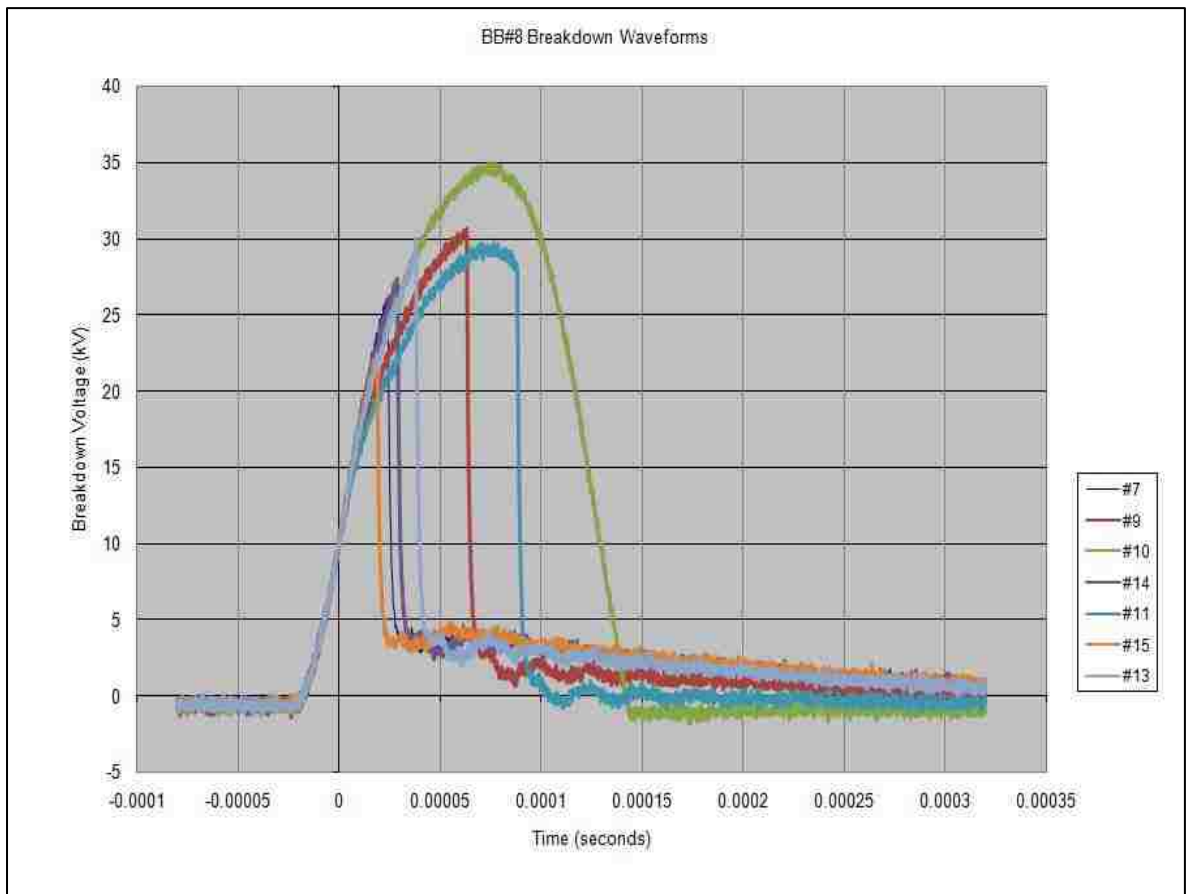


Fig. 5.9: BB#8 Breakdown Waveforms.

Fig. 5.10 shows the Weibull plot of 7 good data points collected from the ceramic/epoxy composite material part - BB#8 which underwent high voltage pulsed power breakdown tests. The data shows an excellent fit to the Weibull 2-parameter function.

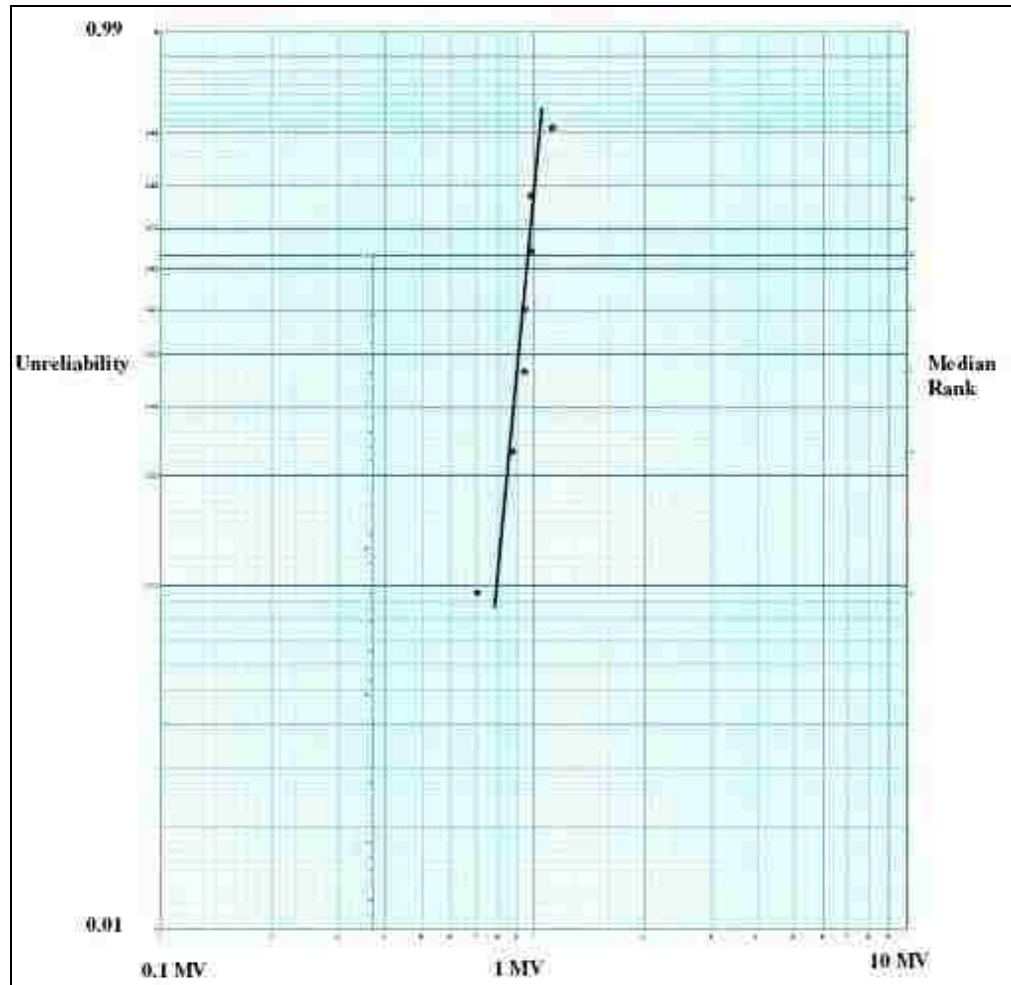


Fig. 5.10: Weibull plot of the HV DC breakdown test for part – BB#8.

Table 5.6 shows test sample data for part – BB#9. Five samples out of 16 were good data points. The average breakdown field is approximately 0.76 MV/cm and the standard deviation is approximately 0.2 MV/cm.

Table 5.6: Test sample data for part – BB#9.

Rank	Sample #	kV/mil	MV/cm	Thickness (mils)	V (kV)
1	13	2.59	0.36	15	13.8
2	9	1.88	0.74	15	28.2
3	2	2	0.79	15	30
4	10	2.4	0.91	15	34.8
5	6	2.5	1.02	15	38.8

Fig. 5.11 shows breakdown waveforms for part – BB#9. Again, the rise times for each sample are very similar and follow an LC tank circuit until the sample breaks down. The capacitance values must be very close between samples. Notice sample #13 broke down very early.

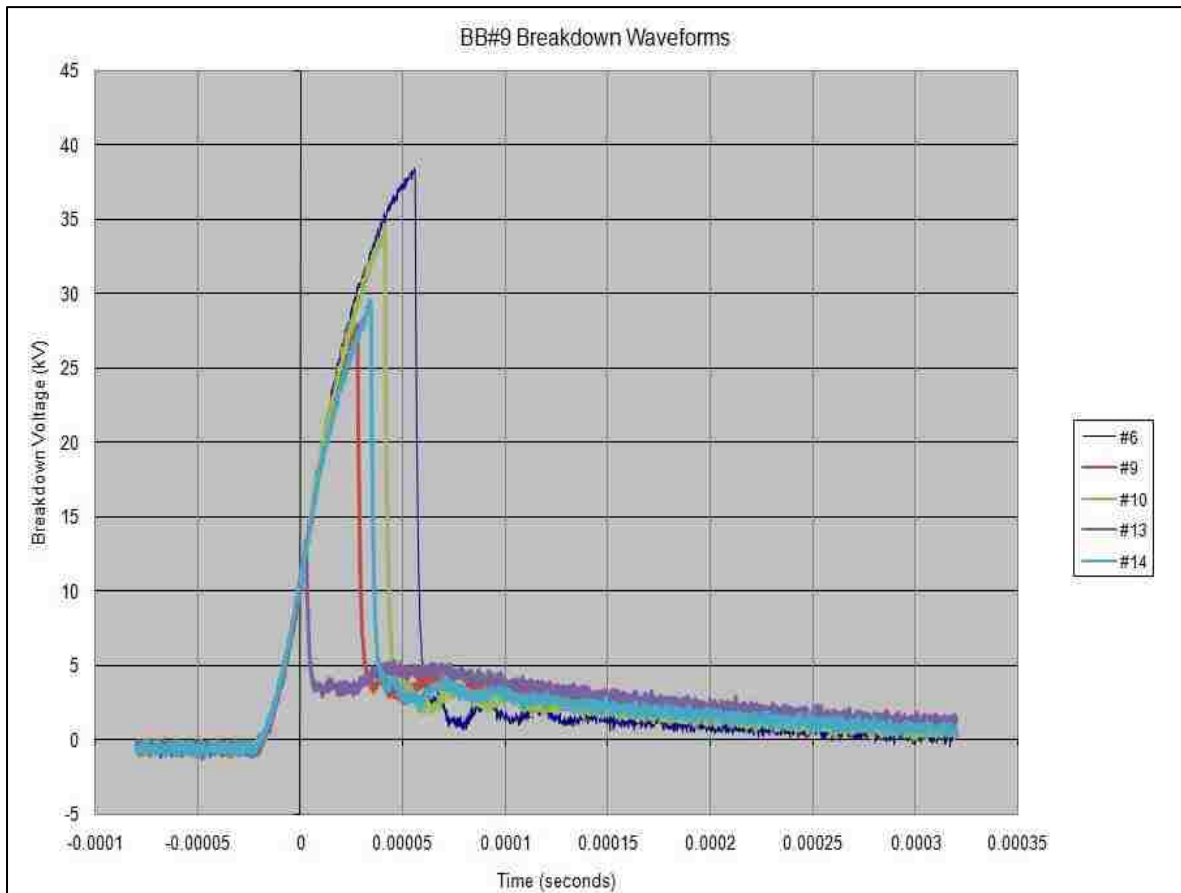


Fig. 5.11: BB#9 breakdown waveforms.

Fig. 5.12 shows the Weibull plot of 5 good data points collected from the ceramic/epoxy composite material part - BB#9 which underwent high voltage pulsed power breakdown tests.

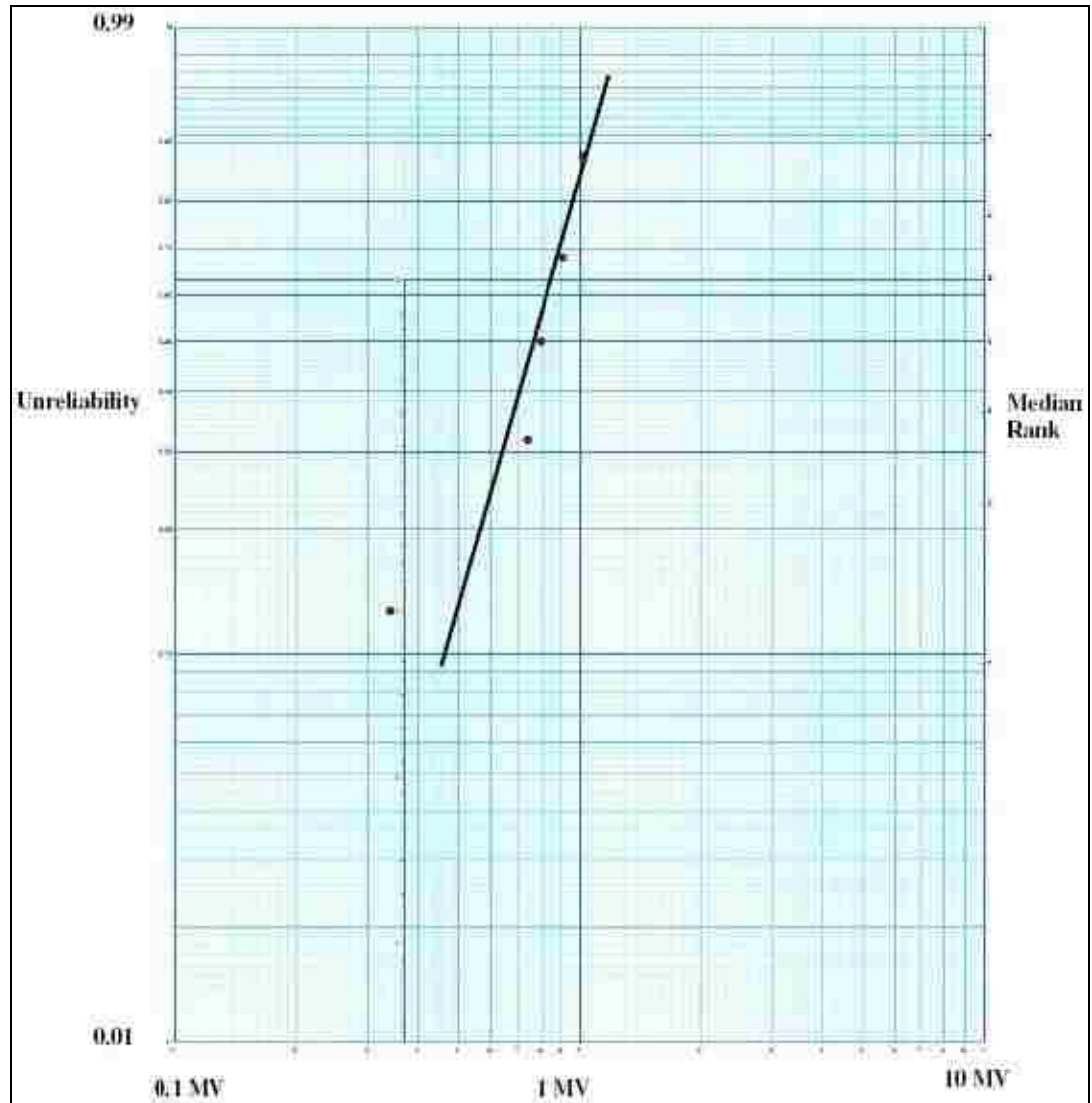


Fig. 5.12: Weibull plot of the HV DC breakdown test for part – BB#9.

Table 5.7 shows test sample data for part – BB#10. Seven samples out of 16 were good data points. The average breakdown field is approximately 0.93 MV/cm and the standard deviation is approximately 0.13 MV/cm.

Table 5.7: Test sample data for part – BB#10.

Rank	Sample #	kV/mil	MV/cm	Thickness (mils)	V (kV)
1	14	2.09	0.82	14.5	30.4
2	6	2.16	0.85	14	30.2
3	8	2.18	0.86	15.5	33.8
4	12	2.32	0.91	15.5	36
5	11	2.39	0.94	14	33.4
6	10	2.5	0.98	14	35
7	13	2.9	1.14	14	40.6

Fig. 5.13 shows breakdown waveforms for part – BB#10. Again, the rise times for each sample are very similar and follow an LC tank circuit until the sample breaks down. It can be seen from the rise time that the capacitance values must be very close between samples. Notice sample #10 and sample #13 appear to not have broken down. This is not the case. Additional shots were taken on the samples and did not hold any voltage.

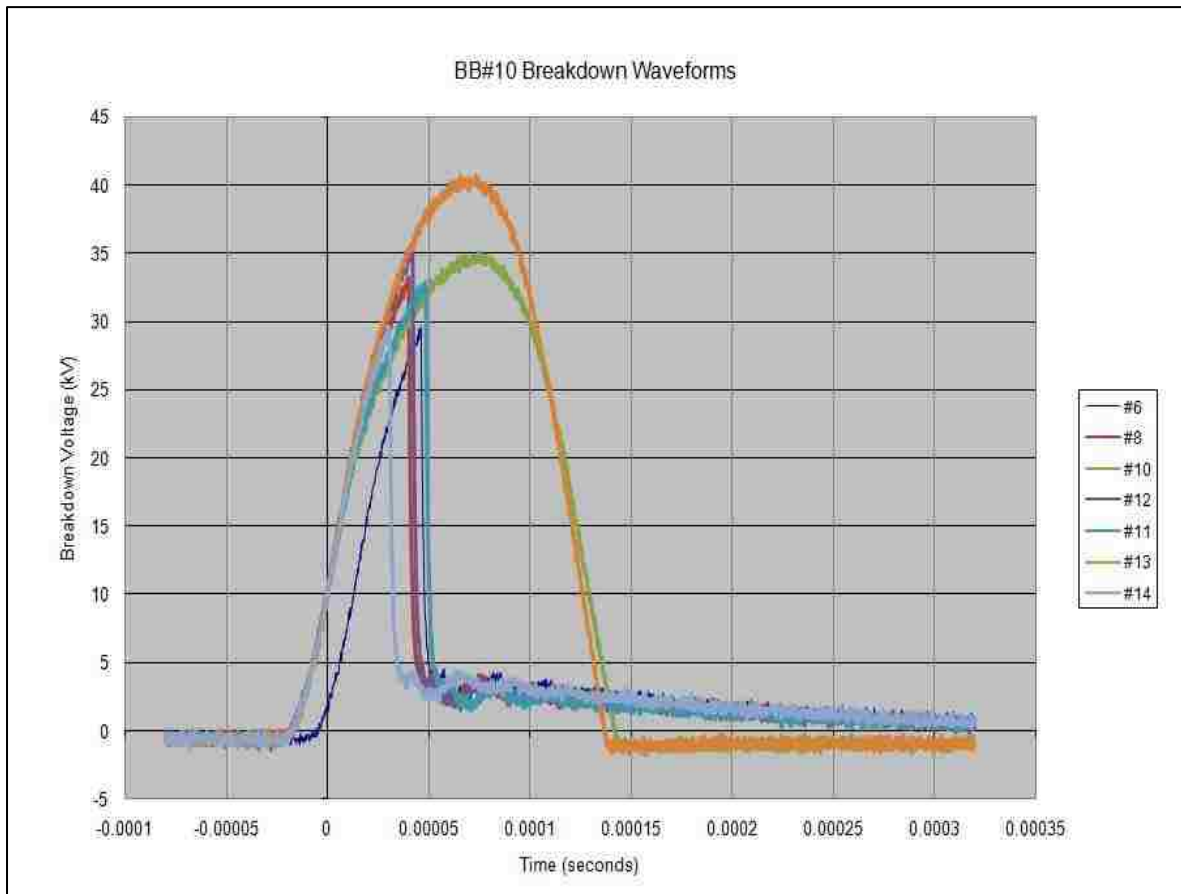


Fig. 5.13: BB#10 breakdown waveforms.

Fig. 5.14 shows the Weibull plot of 7 good data points collected from the ceramic/epoxy composite material part - BB#10 which underwent high voltage pulsed power breakdown tests. The data shows the goodness of the fit with the Weibull function.

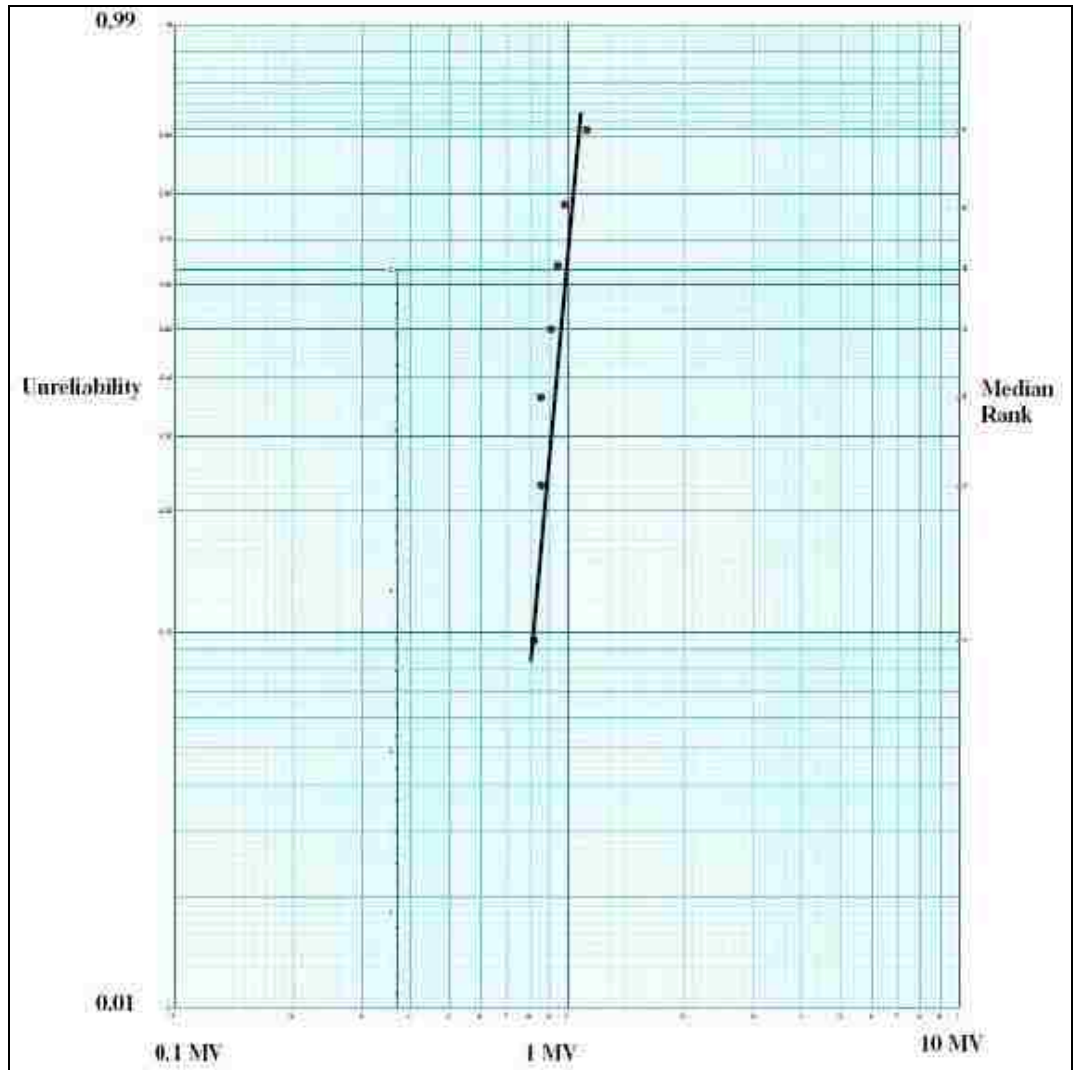


Fig. 5.14: Weibull plot of the HV DC breakdown test for part – BB#10.

Table 5.8 shows test sample data for part – BB#11. Five samples out of 16 were good data points. The average breakdown field is approximately 0.84 MV/cm and the standard deviation is approximately 0.06 MV/cm.

Table 5.8: Test sample data for part – BB#11.

Rank	Sample #	kV/mil	MV/cm	Thickness (mils)	V (kV)
1	6	1.859	0.73	17	31.6
2	8	1.95	0.77	16.5	32.2
3	14	2.2	0.87	15	33
4	3	2.29	0.90	14.5	33.2
5	15	2.29	0.90	16.5	37.8

Fig. 5.15 shows breakdown waveforms for part – BB#11. Again, the rise times for each sample are very similar and follow an LC tank circuit until the sample breaks down. It can be seen from the rise time that the capacitance values must be very close between samples.

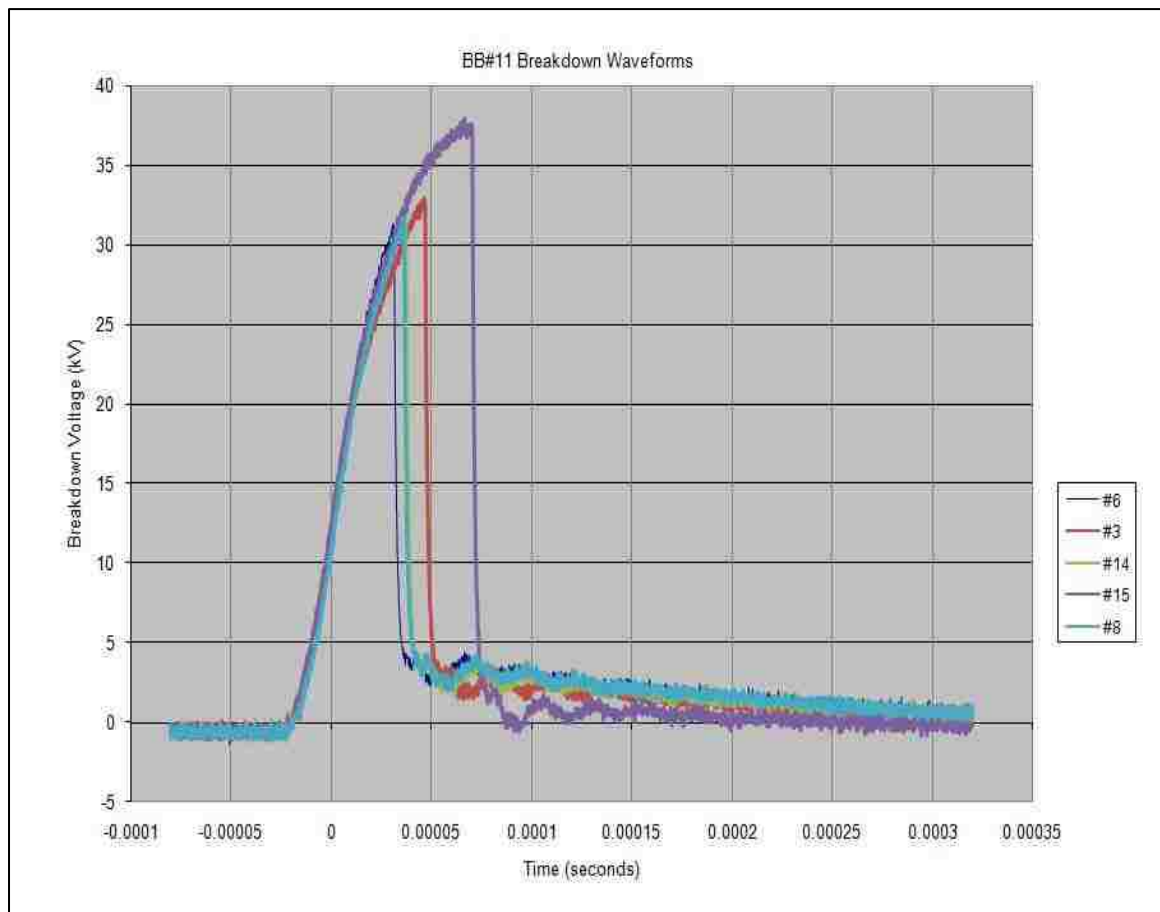


Fig. 5.15: BB#11 breakdown waveforms.

Fig. 5.16 shows the Weibull plot of 5 good data points collected from the ceramic/epoxy composite material part - BB#11 which underwent high voltage pulsed power breakdown tests.

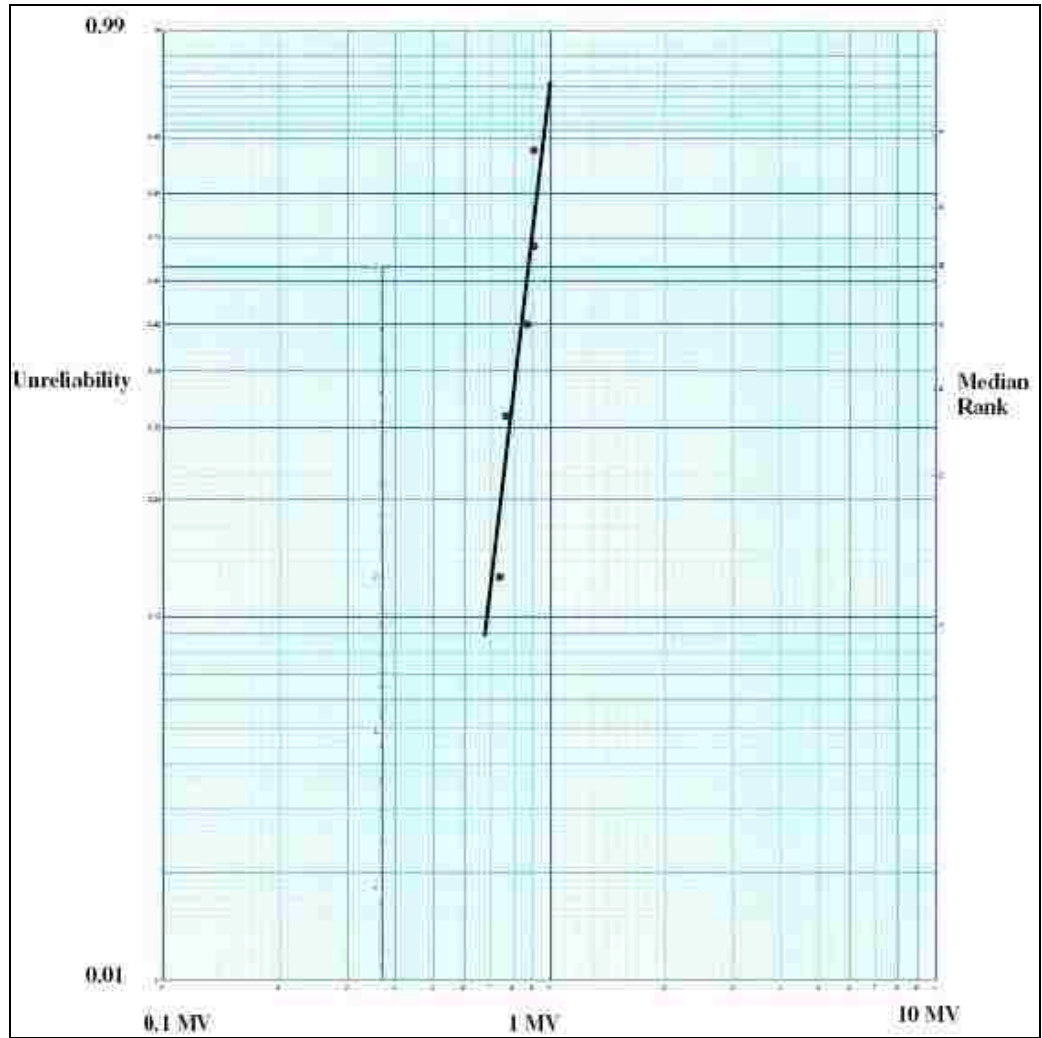


Fig. 5.16: Weibull plot of the HV DC breakdown test for part – BB#11.

The small standard deviation for each part shows that the ceramic/epoxy composite material breaks down consistently at a critical electrical field. The steepness of the slope (β) indicates the likelihood of failure increases rapidly as the electric field applied to the sample gets larger.

With the data combined for BB#8 and BB#10 considering the different thickness between the precision ball bearings (gap distance containing the ceramic/epoxy composite material), it was calculated that the average electrical field breakdown was 2.4 kV/mil with a deviation of 0.33 kV/mil or 0.93 MV/cm with a deviation of 0.13 MV/cm. Also, with the data combined for BB#9 and BB#11 considering the different thickness between the precision ball bearings (gap distance containing the ceramic/epoxy composite material), it was calculated that the average electrical field breakdown was 2.03 kV/mil with a deviation of 0.79 kV/mil or 0.80 MV/cm with a deviation of 0.31 MV/cm.

The data for BB#8 and BB#10 were combined separately from BB#9 and BB#11 because of the slight differences in electrical breakdown fields between them. This can be noticed by looking at the electrical breakdown fields in the tables and also by the significant difference in average electrical field breakdown and standard deviation calculated for the combined parts. This shows that the parts may have had differences in which they were processed. BB#9 and BB#11 had more flaws than BB#8 and BB#10 since the average electrical breakdown field was lower than BB#8 and BB#10 and the standard deviation was greater than BB#8 and BB#10.

CHAPTER 6: SUMMARY AND CONCLUSIONS

6.1 Summary

The studies of the dielectric breakdown of ceramic materials such as micron sized titania, dense titania, and ceramic/epoxy composite materials under pulsed power conditions are important. The research described in this thesis can move present technology to the state-of-the-art because it can reduce the size and weight of a system and provide average power capability with much greater reliability [15]. Before this can occur, the much-desired material has to be identified. This can only be done through research.

Overall, the test results show that dense titania ceramics breakdown at higher voltages than micron size titania. This is due to decreased voids and flaws in the material. As thickness is increased in dense titania, more voids and flaws are introduced and the likelihood of high voltage breakdown increases.

It was observed that dense titania breaks down at lower voltages when pulsed power is applied than when DC ramp is applied. A quick investigation showed the same for mylar to affirm this possibility.

More research into the dielectric breakdown of ceramic materials and the possibility of finding a material with increased breakdown strength than dense titania led to the testing of barium titanate materials. The barium titanate materials researched turned out to be a composition between an epoxy and ceramic materials. The use of epoxy with ceramic materials was to decrease voids and flaws by filling in the voids and flaws with epoxy.

Recent research on the suppression of streamer velocity in transformer oil using nanoparticles suggests that possibly a similar mechanism might explain the results observed with our dielectrics, although this is premature [28].

Both types of material, dense titania and ceramic/epoxy composites, underwent high voltage ramp testing and high voltage pulsed power testing in attempts to characterize the voltages the materials broke down at. After comparing the high voltage DC ramp test data from the micron size TiO_2 , the dense titania, and the ceramic/epoxy composite material, it can be seen that the ceramic/epoxy composite material outperforms the titania materials. The ceramic/epoxy composite material has greater electrical breakdown strength. Dense titania has an average electric breakdown field of 728 kV/cm while the ceramic/epoxy composite material has an average electric breakdown field of 2.55 MV/cm using Weibull statistics. Using Weibull statistics, the test data also shows that there is a standard deviation of 0.14 MV/cm electrical breakdown field between the ceramic/epoxy composite material samples. The small standard deviation shows that the ceramic/epoxy composite material breaks down consistently at a critical electrical field. This is more reliable than dense titania.

High voltage pulsed power test data between the dense titania and ceramic/epoxy composite material were compared. This would be reasonable since the dense titania material has decreased electrical breakdown strength when high voltage pulsed power is applied compared to high voltage DC ramp. This is due to different electrical breakdown effects from DC charged solids and pulsed charged systems [14]. After comparing the high voltage pulsed power test data from dense titania and ceramic/epoxy composite material, it can be seen that the ceramic/epoxy composite material outperforms the dense

titania materials. The ceramic/epoxy composite material has greater electrical breakdown strength. Dense titania has an electric breakdown field of 790 kV/cm. This test data was obtained from a batch of two samples where the dense titania sample with the highest electrical breakdown field was chosen. An average was not used for dense titania where high voltage pulsed power was applied. Ceramic/epoxy composite material has an average electrical breakdown field of 930 kV/cm. For ceramic/epoxy composite material, the best average electrical breakdown field and standard deviation out of the two combined sets of parts was chosen. This information was found using Weibull statistics. Using Weibull statistics, the test data also shows that there is a standard deviation of 0.13 MV/cm electrical breakdown field between the ceramic/epoxy composite material samples. The small standard deviation shows that the ceramic/epoxy composite material breaks down consistently at a critical electrical field. This is more reliable than dense titania. Also note that an average electrical breakdown field for ceramic/epoxy composite material was used for comparison as compared to dense titania where the dense titania sample with the highest electrical breakdown field was chosen.

6.2 Conclusions

High voltage DC ramp tests and high voltage pulsed power tests were performed on several samples of micron sized titania, dense titania, and ceramic/epoxy composite materials. After examining the waveforms, reviewing the data, and applying Weibull statistics where possible; a conclusion can be drawn that the ceramic/epoxy composite materials fared better than the micron sized titania samples and the dense titania samples. The ceramic/epoxy composite materials maintained the highest electrical breakdown fields under both high voltage DC ramp tests and high voltage pulsed power tests. The

ceramic/epoxy composite materials also proved to be more reliable than the micron sized titania samples and the dense titania samples by consistently breaking down at certain electrical fields. The spread of the breakdown fields for the dense titania samples were sporadic and there were insufficient samples to find out how reliable the material can be.

The search for material that has high dielectric constant, high breakdown strength, and can survive numerous amounts of discharges would be beneficial in the field of high voltage pulsed power. There are many applications. One application is Blumlein lines. Research for Blumleins lines is being done by the University of New Mexico to see how they can be made more compact.

Fig. 6.1 shows various methods for Blumleins: a basic Blumlein line, a stacked Blumlein line, and a folded Blumlein line [2]. These are typical methods used today.

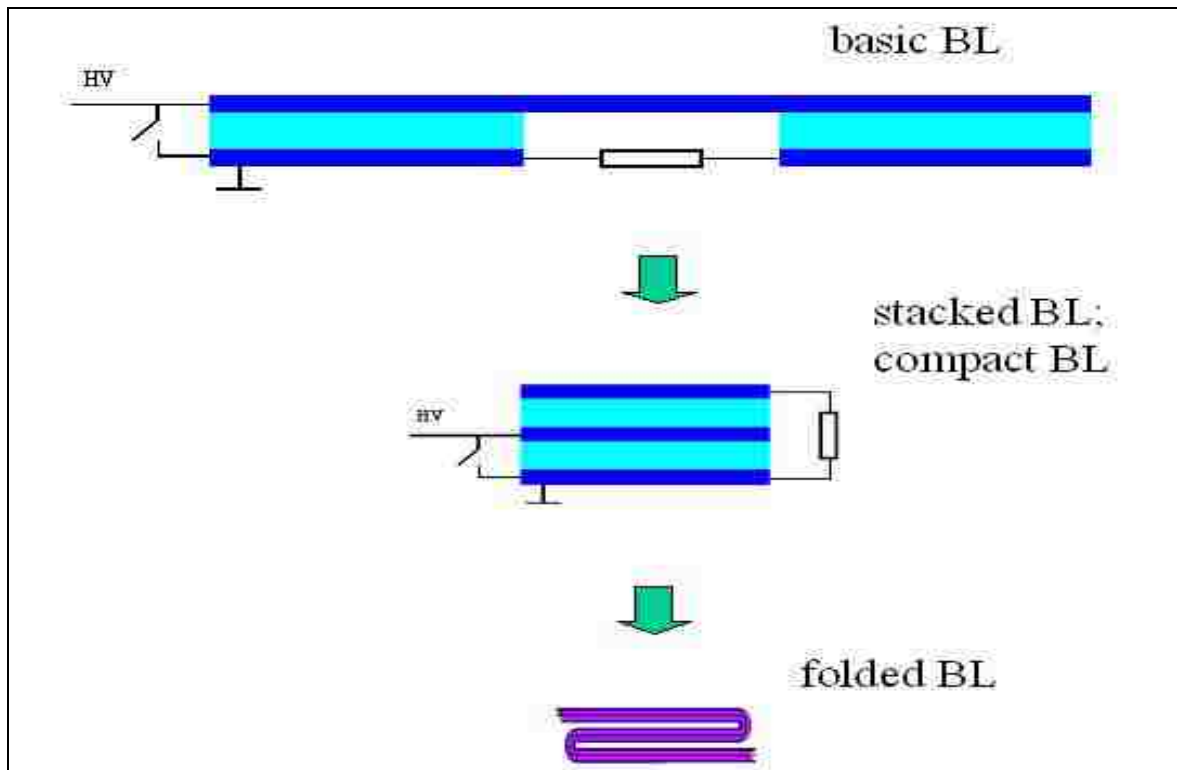


Fig. 6.1: Sketches of the basic Blumlein line, stacked Blumlein line, folded Blumlein line.

Any methods used to compact Blumlein lines by stacking and folding with the use of standard dielectric materials still proves to be costly, complex, inefficient and bulky.

Fig. 6.2 shows a folded Blumlein line and a straight Blumlein line. The folded or bent Blumlein line would be compact but would still be very long. This is because the dielectric constant of the material between the lines would be low but would have high breakdown strength. This is a more traditional Blumlein line, which is present technology except that it would be folded.

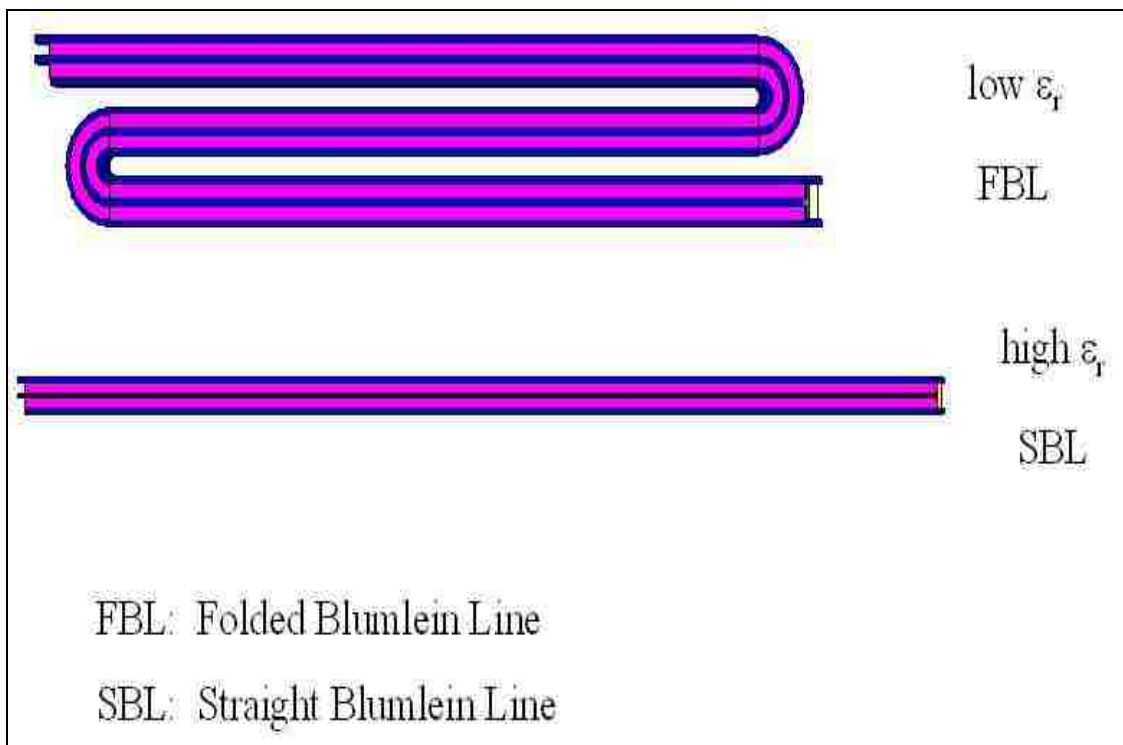


Fig. 6.2: Sketches of the folded Blumlein line and straight Blumlein line.

With the use of a material such as ceramic/epoxy composite material, the straight Blumlein line would be compact and would be shorter in length. This is because the dielectric constant of the material between the lines would be high and would have high breakdown strength. Also, the straight Blumlein line would be able to survive numerous amounts of discharges as compared to the folded or bent Blumlein line because folds or

bends in the folded or bent Blumlein line can present a good chance for high voltage breakdown.

In moving research forward, the University of New Mexico is also involved in investigating the behavior of the dielectric constant of composite material as the ceramic materials generally present a nonlinear dependence. The dielectric constant varies as a function of applied voltage. There has been a paucity of research on this nonlinear behavior for ceramic composites and it is necessary to understand the ϵ variation for two basic applications in pulsed power: linear & nonlinear transmission lines (NLTLs) [29].

REFERENCES

- [1] S.T. Pai & Qi Zhang, *High Power Pulse Technology*, World Scientific Publishing Co. Pte. Ltd., 1995.
- [2] M. Joler, C. Christodoulou, J. Gaudet, E. Schamiloglu, "Effects of Bending in a Stacked, Parallel-plate Blumelein Pulse-forming Line," 31st IEEE International Conference on Plasma Science, June 28-July 1, 2004, Baltimore, Maryland.
- [3] F. F. Chen, *Introduction to Plasma Physics and Controlled Fusion Volume 1: Plasma Physics*, Second Edition, Plenum Press, 1984.
- [4] D. C. Giancoli, *Physics Principles with Applications*, Fourth Edition, Prentice Hall, 1995.
- [5] F. T. Ulaby, *Fundamentals of Applied Electromagnetics*, Prentice-Hall Inc., 2001.
- [6] K. C. Kao, *Dielectric Phenomena in Solids*, Elsevier Academic Press, 2004.
- [7] M.W. Barsoum, *Fundamentals of Ceramics*, IOP Publishing, 2003.
- [8] C. T.A. Johnk, *Engineering Electromagnetic Fields and Waves*, Second Edition, Wiley, 1988.
- [9] J. A. Edminister, *Schaum's Outline of Theory and Problems of Electromagnetics*, Second Edition, McGraw-Hill, 1993.
- [10] M.Y. Koledintseva, S. K. Patil, R.W. Schwartz, W. Huebner, K.N. Rozanov, J. Shen, J. Chen, " Prediction of Effective Permittivity of Diphasic Dielectrics as a Function of Frequency," IEEE Transactions on Dielectrics and Electrical Insulation vol. 16, No. 3, June 2009.
- [11] J.C. Martin, "Nanosecond Pulse Techniques," Proceedings of the IEEE vol. 80, No. 6, June 1992.

- [12] T.H. Martin, A.H. Guenther, M. Kristiansen, *Advances in Pulsed Power Technology Volume 3: J.C. Martin on Pulsed Power*, Plenum Press, 1996.
- [13] Weibull information, <http://www.weibull.com>.
- [14] M.W. Barsoum, *Fundamentals of Ceramics*, IOP Publishing, 2003.
- [15] E. Schamiloglu, K.H. Schoenbach, R.J. Vidmar, "On the Road to Compact Pulsed Power: Adventures in Materials, Electromagnetic Modeling, and Thermal Management," IEEE, 2003.
- [16] P. Castro, C.J. Buchenauer, J. Gaudet, and E. Schamiloglu, "Studies of Dielectric Breakdown under Pulsed Power Conditions," 2005 IEEE International Pulsed Power Conference, 2005, Monterrey, California.
- [17] A. El Gorsey, M. Chen, L. Dubrovinsky, P. Gillet, G. Graup, "An Ultradense Polymorph of Rutile with Seven-Coordinated Titanium from the Ries Crater," *Science*, 2001, 293, 5534, 1467 – 1470 doi:10.1126/science.1062342, (<http://dx.doi.org/10.1126/science.1062342>).
- [18] A. El Gorsey, M. Chen, P. Gillet, L. Dubrovinsky, G. Graup, R. Ahuja, "A Natural Shock-Induced Dense Polymorph of Rutile with α -PbO₂ Structure in the Suevite from the Ries Crater in Germany," *Earth and Planetary Science Letters*, 192, 4, 2001, 485-495, doi:10.1016/S0012-821X(01)0048-0, ([http://dx.doi.org/10.1016/S0012-821X\(01\)00480-0](http://dx.doi.org/10.1016/S0012-821X(01)00480-0)).
- [19] E. J. Schultz, *Fully Exploiting the Potential of the periodic Table Through Patter Recognition*, Chem. Educ. 2005 82 1649.
- [20] N. N. Greenwood, A. Earnshaw, *Chemistry of the Elements* (2nd ed.), Oxford:Butterworth-Heinemann, ISBN 0-7506-3365-4, 1997.

- [21] J. Emsley, *Nature's Building Blocks: An A-Z Guide to the Elements*, Oxford: Oxford University Press, pp. 451-53. ISBN 0-19-850341-5, 2001.
- [22] Electronic Materials, <http://www.tplinc.com>.
- [23] Toxicological Profile for Barium and Barium Compounds. Agency for Toxic Substances and Disease Registry, CDC. 2007. [1] (<http://www.atsdr.cdc.gov/toxprofiles/tp24.pdf>).
- [24] Toxicity Profiles, Ecological Risk Assessment | Region 5 Superfund | US EPA, (<http://www.epa.gov/region5/superfund/ecology/html/toxprofiles.htm#ba>).
- [25] "Nanoparticle Compatibility: New Nanocomposite Processing Technique Creates More Powerful Capacitors", (<http://gtresearchnews.gatech.edu/newsrelease/barium-titanate.htm>).
- [26] E. K. Nyutu. "Effect of Microwave Frequency on Hydrothermal Synthesis of Nanocrystalline Tetragonal Barium Titanate". *The Journal of Physical Chemistry C* 112: 9659.doi:10.1021/jp7112818, 2008.
- [27] Weibull plotting paper provided at <http://pharm.kuleuven.be/pharbio/gpaper.htm>.
- [28] J.G. Hwang, F. O'Sullivan, M. Zahn, O. Hjortstam, L.A.A. Petterson, R. Liu, "Modeling of Streamer Propagation in Transformer Oil-Based Nanofluids," Annual Report Conference on Electrical Insulation Dielectric Phenomena, 2008.
- [29] J.O. Rossi, P. Castro, M. Roybal, E. Schamiloglu, "High-Voltage Energy Store in Organic Composite Dielectrics for Compact Pulsed Power," University of New Mexico.